STATISTICAL STUDIES OF DM DOMINATED SUBHALOS

By

Kifelom Mehari

A THESIS PRESENTED TO

THE PROGRAM OF GRADUATE STUDIES
ADDIS ABABA UNIVERSITY

IN PARTIAL FULFILLMENT OF THE REQUIREMENTS
FOR THE DEGREE

MASTER OF SCIENCE in PHYSICS

ADDIS ABABA, ETHIOPIA

OCTOBER 2018

ADDIS ABABA UNIVERSITY

PROGRAM OF GRADUATE STUDIES

STATISTICAL STUDIES OF DM DOMINATED SUBHALOS

By

Kifelom Mehari

Deparment of Physics

Addis Ababa University

Approved by the Examining Board:

Dr. Remudin Reshid Signature _____
Advisor

Dr. Deribe Hirpo Signature _____
Examiner

Dr. Getinet Feleke Signature _____
Examiner

Dated: October 2018

ADDIS ABABA UNIVERSITY

Date: **October 2018**

Author: **Kifelom Mehari**

Title: **Statistical Studies of DM Dominated Subhalos**

Department: **Deparment of Physics**

Degree: **M.Sc.** Convocation: **october** Year: **7**

This Work is Dedicated

to

Mum, Dad, my wife, Ergotism victims in wollo in 1966/1973 and to the European helicopter pilots who brought them to Dessie hospital.

Table of Contents

List of Tables

List of Figures

Acknowledgements

ACKNOWLEDGMENTS

I would like to express my sincere gratitude to my advisor Dr. Remudin Reshid for the continuous guidance and great support.

I am also express my great acknowlegement to the best teachers Dr. Mirjana povich, Dr. Hailezge, Dr. Mulugeta, Dr. Fissha, Dr Teshome, Dr. Tateke, Dr. Belayneh, Dr. Derebe, Dr. Tilahun and Dr. Cherenet.

I also thanks my colleagues especially to Abdu, Tilahun, Zeleke and Shambelu for their collaboration.

I am also highly grateful and thanks to my wife Hirut Tefera.

Special thanks to God and his son Jesus Christ.

Addis Ababa University Kifelom Mehari

July, 2018

Acronyms and Abbreviations Used

χ	=	lightest neutralino, a supersymmetric dark matter candidate
G	=	gravitino, a supersymmetric dark matter candidate
GMSB	=	gauge-mediated supersymmetry breaking
KK	=	kaluza klein particle
LKP	=	lightest Kaluza-Klein particle
LSP	=	lightest supersymmetric particle
NLSP	=	next-to-lightest supersymmetric particle
G_N	=	Gravitational constant
M_{pl}	=	Planck mass$\simeq 1.2 \times 10^{19} GeV$
M_*	=	reduced Planck mass$\simeq 2.4 \times 10^{18} GeV$
DE	=	Dark energy
MSSM	=	supersymmetric standard model with minimal number of extra particles
SM	=	standard model of particle physics
stau	=	scalar superpartner of the tau lepton
superWIMP	=	superweakly-interacting massive particle
UED	=	universal extra dimensions
WIMP	=	weakly-interacting massive particle
X	=	general dark matter candidate
AHF	=	Amiga Halo Finder
FOF	=	Friend of Friends
CMB	=	Cosmic microwave background
BBN	=	Big Bang Nucleosynthesis
CMBR	=	Cosmic Microwave Background Radiation
DM	=	Dark Matter

CDM	=	Cold Dark Matter
ALPs	=	Axion like particles
LEP	=	Large electron proton
SZ	=	Sunyaev Zeldovich effect
tSZE	=	Thermal Sunyaev Zeldovich Effect
NFW	=	Navarro,Frenk and White
BDM	=	Bound density maximum
SUBFIND	=	Subhalo finder
ROCKSTAR	=	Robust overdensity calculation
		using k space Topological Adaptive Refinement
SHMFs	=	Subhalo mass functions
AMR	=	Adaptive mesh refinement
SURV	=	subhalos with Viral radius
SHVFs	=	Subhalo velocity functions
CP	=	Charge parity
MACHOs	=	Massive Astrophysical compact halo objects
CSAI	=	Computer Simulation Assisted Instruction
CSE	=	Computer Simulated Experiment
AAU	=	Addis Ababa University

Abstract

Abstract

The content of the universe is highly dominated by dark matter (DM). We can identify it using gravitational lensing and it may be detected using direct method, after scattered with the nuclie of germanium which is held underground and indirect method, after annihilation into electron or positron, which shows a scientilation effect. The viable candidates of DMs are weakly interacting particles (WIMPS), Axions, MACHOS, Sterile Neutrinos, superWIMPS and gravitinos. All these candidates are studied under super symmetric model, which is the extension of standard model. In these thesis we are focusing on statistical studies of DM dominated subhalos. We will describe the statistical distribution of DM using ROCKSTAR halo finders. Using marenostrum-multidark simulation of galaxy Clusters, we analyse mass to light ratio of the clusters in $\frac{r}{r_{200}}$. So the mass to light ratio is high at $\sim r_{200}$. These show that the concentration of DM halos is high at radius of r_{200}. From the statistical studies of all the subhalos we have found that the radial distribution of the mass to light DM subhalos is more strongly peaked at r_{200}. These may suggest that the search for content of DM from subhalos in clusters is most promising at r_{200}. We also determine the DM fraction for five different clusters with in 30 kpc and the minimum number of particle is 100. We also compare its value with in 15 kpc and the minimum number of particle is 50. We found that the statistical distribution of sub halo is high in 15 kpc than in 30 kpc. But in both cases the concetration of DM is high with in a mass of $1 - 10 \times 10^{10} M_0$. In our simulation we are focusing on ROCKSTAR halo finder, but still there are different types of halo finders such as Amiga halo finder, body density maximum algorithm, surv finder, SUBFIND algorithm and FOF based algorithm. In all condition the density distribution of DM is gaussian distribution. We also analyse the existence of DM by using generalized viral theorm in $f(R)$ gravity. It helps to show that the mass of DM is dominant in the cluster. Non interacting mathematical model of DM

is also emphasized in this thesis, which is trying to show that, DM particles are non interacting and gravitationaly bound in the cluster of halos and its subhalos.

Introduction

The invisible part of the universe is known as Dark matter. Our universe is not only consists of baryonic matter such as gas and luminous object, it also contains non baryonic particle, which is the main candidates of dark matter. It is analyzed beyond standard model, which is supersymmetric model. In supersymmetric model, we expect that, dark matter consists of bosons W^+ and W^- and Higgs bosons b [1].

Only about 4% of the mass-energy content of the universe is composed of ordinary baryonic matter, the bulk of which is diffuse gas rather than stars and galaxies. The matter visible to us in current telescopes only represents a small fraction of the total amount present in the Universe. Most of the matter instead appears to be in some form which does not emit light, or at least very little. This is what is referred to as dark matter. There is a strong evidence for significant amount of non luminous matter in the universe referred to as Dark matter.

The first detection of dark matter is attributed to Zwicky, who measured the velocity dispersion of galaxies in the Coma cluster and found their velocities to be far exceed that which could be attributed to the luminous matter in the galaxies themselves. The work of Zwicky on Coma cluster was followed up by Smith for the Virgo cluster of galaxies. Once again, the velocities of its constituent galaxies indicated an unexpectedly high mass-to-light ratio [2].

Dark matter makes up about 23% of mass-energy of the universe. Thus the total mass energy is 23% dark matter plus 4% baryons, for total 27%, but the remaing about 73% is carried by the so-called dark energy, that is mostly observed through its accelerating effect on the expansion of the universe as observed, e.g., by comparing the luminosity distance and the redshift of distant supernovae. Evidence for excess gravitational acceleration that cannot be explained by observable matter has been found on both small, galactic scales and large, cosmological scales. If Newton's law of gravity, or general relativity, is valid, then the universe must contain a constituent of unknown nature that betrays its presence only through

gravitation. If so, the absence of a radiative signal or excess scattering of baryonic matter requires that those particles be uncharged and at most weakly interacting. Numerous candidate particles have been proposed over the years, and a hunt is on to detect them directly via elastic scattering in laboratory devices or indirectly through an astronomical decay or annihilation signal [3].

Several observations suggest that most of the matter in the universe is dark and non-baryonic. Various methods based on direct or indirect detection have been proposed to constrain the nature and the properties of the Dark Matter (DM). A promising way to study the DM properties consists in the detection of the electromagnetic emissions coming from astrophysical objects as a consequence of DM particles annihilation and secondary particle electron or positron production, because the spectral features of these emissions are expected to be closely correlated with the nature. Its composition help us to determine the mass of the DM particles [5].

The first strong indications of dark matter in dwarf galaxies came in the early 1980s. Faber and Lin (1983) studied dwarf spheroidals and found them to contain large amounts of dark matter. Subsequent studies have in fact shown that dwarf galaxies have higher mass-to-light ratios than normal galaxies.

In the 1970s, Vera Rubin and collaborators and Albert Bosma measured the rotation curves of individual galaxies and also found evidence for non-luminous matter. This and other classic evidence for non-luminous matter has now been supplemented by data from weak and strong lensing, hot gas in clusters, the Bullet Cluster, Big Bang nucleosynthesis (BBN), further constraints from large scale structure, distant supernovae and the cosmic microwave background radiation (CMBR). Together, these data now provide overwhelming evidence for the remarkable fact that not only is there non-luminous matter in our Universe, but most of it is composed of non-baryons or any of the other known particles. In addition, dark matter is necessary to explain structure formation, as deduced from the cosmic microwave background measurements. Clumps of neutral particles arose first through gravitational attraction and later, when the neutral atoms were formed, these were gravitationally attracted by the dark matter to form the galaxies. The above analysis of rotation curves implies that 90% of the mass in galaxies is dark.

Current data imply that dark matter is five times more prevalent than normal matter and accounts for about a quarter of the Universe. More precisely, these data constrain the energy densities of the Universe in baryons, non-baryonic dark

matter (DM), and dark energy to be [1]

$$\Omega_B = 0.0456 \pm 0.0016 \tag{1}$$

$$\Omega_{DM} = 0.227 \pm 0.014 \tag{2}$$

$$\Omega_\Lambda = 0.728 \pm 0.015 \tag{3}$$

Despite this progress, all of the evidence for dark matter noted above is based on its gravitational interactions. Given the universality of gravity, this evidence does little to pinpoint what dark matter is.

The existence of Dark Matter (DM) now comes from a number of astrophysical and cosmological probes (such as galaxy rotation curves, weak lensing measurements and the precise data from the Cosmic Microwave Background observations and the Large Scale Structure surveys of the Universe) [6]. The indirect detection strategy relies on the possibility of seeing signals of the presence of DM in terms of the final products $(e^{\pm}, \gamma, \nu ...)$ of DM annihilations in the galactic halo, on top of the ordinary cosmic rays. Dark matter is not antimatter, because we do not see the unique gamma rays that are produced when antimatter annihilates with matter. We can also rule out large galaxy sized black holes on the basis of how many gravitational lenses we see. High concentrations of matter bend light passing near them from objects further away, but we do not see enough lensing events to suggest that such objects to make up the required 23% dark matter contribution.

The recent positive results from a number of indirect detection experiments have suggested the possibility that indeed such a signal has been seen. In particular, the signals point to an excess of electrons and positrons. DM particle of any mass (above about $100GeV$) that annihilates only into leptons $(DMDM \to e^+e^-, \mu^+\mu^-, \tau^+\tau^-)$ or a DM particle with a mass around or above $1TeV$, that can annihilate into any channel (i.e.$DMDM \to W^+W^-, ZZ, bb', tt'$ light quark pairs and leptonic channels) [4].

In any case, a very large annihilation cross section is needed: of the order of $10^{-23}cm^3/sec$ up to $10^{-20}cm^3/sec$ or more, depending on the mass of the candidate and the annihilation channel. These numbers are much larger than the typical cross section required by DM thermal production in cosmology $\sim 3 \times 10^{-26}cm^3/sec$.

Most scientists think that dark matter is composed of non-baryonic matter. The lead candidate, WIMPS (weakly interacting massive particles), have ten to a hundred times the mass of a proton, but their weak interactions with normal matter make them difficult to detect. Neutralinos, massive hypothetical particles heavier

and slower than neutrinos, are the foremost candidate, though they have yet to be spotted. Sterile neutrinos are another candidate of DM. Neutrinos are particles that don't make up regular matter. A river of neutrinos streams from the sun, but because they rarely interact with normal matter, they pass through the Earth and its inhabitants.

There are three known types of neutrinos; a fourth, the sterile neutrino, is proposed as a dark matter candidate. The sterile neutrino would only interact with regular matter through gravity. The smaller neutral axion and the uncharched photinos are also potential placeholders for dark matter [7].

Albert Einstein showed that massive objects in the universe bend and distort light, allowing them to be used as lenses. By studying how light is distorted by galaxy clusters, astronomers have been able to create a map of dark matter in the universe. All of these methods provide a strong indication that most of the matter in the universe is something yet unseen.

CHAPTER 1

Dark Matter Candidate

1.1 Dark matter particles

We believe and have found some of DM particles are, subatomic particles, or fundamental particles, which having no size and can have no substructure. We are now seeking to explain the properties of these particles and working to show how these can be used to explain the contents of the universe.

There are two types of fundamental particles: matter particles, some of which combine to produce the world about us, and force particles, one of which, the photon, is responsible for electromagnetic radiation. These are classified in the standard model of particle physics and how the basic building blocks of matter interact, which is governed by fundamental forces. Matter particles are fermions while force particles are bosons. Matter particles are split into two groups: quarks and leptons, there are six of these, each with a corresponding partner [4]. Leptons are divided into three pairs. Each pair has an elementary particle with a charge and one with no charge, one that is much lighter and extremely difficult to detect. The lightest of these pairs is the electron and electron-neutrino. The electron-neutrino, is produced copiously in the sun and these interact so weakly with their surroundings that they pass unhindered through the Earth. A million of them pass through every square centimetre of your body every second, day and night.

The particles of the standard model (SM) are divided into three categories [4]:

- Spin $1/2$ Fermions: These matter particles include six flavors of quarks (up, down, Charm, strange, bottom, and top), three flavors of charged leptons (electrons, muons, and taus), and three flavors of neutral leptons (the electron, muon, and tau neutrinos). These are grouped into three generations.
- Spin 1 Gauge Bosons: These force carrying particles include the photon, which mediates electromagnetism; eight gluons g, which mediate the strong nuclear

force; and the W and Z gauge bosons, which mediate the weak inter-actions. The photon and gluons are massless, but the W and Z have masses $80GeV$ and $91GeV$, respectively.

- Spin 0 Higgs Boson: The SM Higgs particle is a spin 0 boson.The Higgs boson is an odd particle: it is the second heaviest of the standard model particles and it resists a simple explanation. It is often said to be the origin of mass. Although the Higgs boson has not yet been discovered, its mass is constrained by a variety of LHP collider results. Assuming the SM, null results from direct searches at the large electron proton (LEP) e^+e^- collider require $M_h > 114GeV$. Given this constraint, precision measurements of electroweak observables at LEP require $M_h < 186GeV$.

The CDM particles are also assumed to [18]

- be collisionless, meaning that they interact through gravity only and have no other significant self-interactions;
- be dissipationless, meaning they cannot cool by radiating photons (as opposed to normal baryonic matter);
- be long-lived, meaning that their lifetimes must be comparable to or longer than the present age of the Universe;
- behave as a perfect fluid on large scales, meaning that the granularity of the DM is sufficiently fine not to to have been directly detected yet through various effects

1.2 Fundamental requirements for dark matter particles

In the following we list three popular types of extensions to the Standard Model in which dark-matter candidates are discussed. An overview over these and other candidates is given as [7]:

1. In supersymmetric extensions of the Standard Model the lightest supersymmetric particle (LSP) is stable on account of a specifc symmetry. Such particles typically have masses above a few GeV and are thus candidates for CDM.

Among these so-called weakly interacting massive particles (WIMPs), one finds the supersymmetric partners of the gauge bosons and the Higgs boson, i.e. a neutralino, LSP of a neutrino, i.e.a sneutrino, or even of the graviton, i.e. the gravitino.

2. Also subsumed as WIMPS are Kaluza Klein excitations found in higher dimensional extensions. Again, the lightest particle of this type can be a dark-matter candidate.

3. Axion like Particles (ALPs) are generally very light, with masses below the MeV scale and typically much less, down to $10^{-9}ev$. In contrast to WIMPs, they are not produced through thermal freeze out, but form a Bose-Einstein condensate with very high occupation numbers. Of particular interest and subject to controversies is the distribution function of dark-matter particles.

1.3 WIMPS and MACHO

1.3.1 WIMPS

WIMPS: Weakly interacting massive particles WIMPS are smaller than atoms. They have mass, but their interactions are so weak that they pass right through ordinary matter. Since each a WIMP has only a small amount of mass, there needs to be a large number of them to make up the bulk of DM. That means that millions of WIMPs are passing through ordinary matter such as the Earth and the Sun every few seconds. Stable weakly interacting massive particles (WIMPs) are attractive cold DM candidates [5].

The WIMPs in our galaxy halo can be gravitationally trapped and accumulated by the Sun and the Earth. They can annihilate into weak bosons and heavy quarks which subsequently decay into neutrinos. Because of their lack of strong interaction with normal matter and lack of interaction through electromagnetism, they would appear dark in current telescopes, unless they happen to decay or annihilate into photons. Although there are no known particles within the standard model of particle physics which correspond to WIMPs, supersymmetric extensions contain a host of potential WIMP candidates.

WIMPs have mass in the range $m_{weak} = 10GeV$ to $1TeV$ and tree-level interactions with W and Z gauge bosons, but not with gluons or photons. WIMPs are the most studied DM candidates, as they are found in many particle physics theories,

naturally have the correct relic density, and may be detected in many ways [6].

WIMPs gravitationally captured by scattering interactions with nucleons in the Sun and Earth could then annihilate and produce a detectable neutrino flux. Once captured, a WIMP continues to scatter, losing energy and sinking to the core of the Sun or Earth; a large abundance of WIMPs can accumulate through this mechanism.

If a WIMP is stable, it is naturally produced with a relic density consistent with that required of DM. DM may be produced in a simple and predictive manner as a thermal relic of the Big Bang. Initially the early Universe is dense and hot, and all particles are in thermal equilibrium. The Universe then cools to temperatures T below the dark exists matter particle's mass M_X, and the number of DM particles becomes Boltzmann suppressed, dropping exponentially as $e^{\left(\frac{-m_x}{T}\right)}$. The number of DM particles would drop to zero, except that, in addition to cooling, the Universe is also expanpanding [6].

In the third stage, the Universe expand and becomes so large and the gas of DM particles becomes so dilute that they cannot find each other to annihilate. The DM particles then freeze out, with their number asymptotically approa-ching a constant to their thermal relic density. Note that freeze out, also known as chemical decoupling, is distinct from kinetic decoupling; after thermal freeze out, interactions that change the number of DM particles become negligible, but interactions that mediate energy exchange between DM and other particles may remain efficient. This process is described quantitatively by the Boltzmann equation [13]

$$\frac{dn}{dt} = -3H_n - < \sigma_A V > (n^2 - n_{eq}^2) \tag{1.1}$$

where n is the number density of the DM particle X, H is the Hubble parameter, $< \sigma_A V >$ is the thermally averaged annihilation cross section, and n_{eq} is the DM number density in thermal equilibrium. On the right-hand side of the above equation, the first term accounts for dilution from expansion. The n^2 term arises from processes $XX \rightarrow SMSM$ that destroy X particles, where SM denotes standerd model particles, and the n_{eq}^2 term arises from the reverse process $SMSM \rightarrow XX$, which creates X particles [6].

The thermal relic density is determined by solving the Boltzmann equation numerically. Defining freeze out to be the time when $n < \sigma_A V >= H$ we have

$$n_f \sim (m_x T_f)^{\frac{3}{2}} \left(\exp\left(\frac{-m_x}{T_f} \right) \right) \tag{1.2}$$

$$n_f \sim \left(\frac{T_f^2}{M_{p1}\langle\sigma_A V\rangle}\right) \tag{1.3}$$

where the subscripts f denote quantities at freeze out. The ratio $x_f = \frac{m_x}{T_f}$ appears in the exponential. It is, therefore, highly insensitive to the DM's properties and maybe considered a constant; a typical value is $x_f = 20$. The thermal relic density is, then,

$$\Omega_x = \frac{m_x n_0}{\rho_c} \tag{1.4}$$

$$\Omega_x = \left(\frac{m_x T_o^3}{\rho_c}\right)\left(\frac{n_o}{T_o^3}\right) \tag{1.5}$$

$$\Omega_x \sim \left(\frac{m_x T_o^3}{\rho_c}\right)\left(\frac{n_f}{T_f^3}\right) \tag{1.6}$$

$$\Omega_x \sim \left(\frac{x_f T_o^3}{\rho_c M_{p1}}\right)\langle\sigma_A V\rangle^{-1} \tag{1.7}$$

Where ρ_c is the critical density and the subscripts 0 denote present day quantities. We see that the thermal relic density is insensitive to the DM mass m_x and inversely proportional to the annihilation cross section $\langle\sigma_A V\rangle$. The annihilation cross section can be written as [3]

$$\langle\sigma_A V\rangle = \kappa\left(\frac{g_{weak}^4}{16\pi^2 m_x^2}\right) \tag{1.8}$$

The constant $g_{weak} \sim 0.65$ is the weak interaction gauge coupling, and κ parameterizes deviations from this estimate. With this parametrization, given a choice of κ, the relic density is determined as a function of m_x . We see that a particle that makes up all of DM is predicted to have mass in the range $m_x \sim 100GeV - 1TeV$; a particle that makes up 10% of DM has mass $m_x \sim 30GeV - 300GeV$. This is the WIMP miracle: weak-scale particles make excellent DM candidates.

1.3.2 The annular modulation signal

If the DM halo of the Milky Way is in the form of WIMPs, the Earth should experience a WIMP wind of such particles as it moves through the halo due to its orbit around the Sun and the orbit of the Sun around the centre of the Galaxy. These WIMPs can in principle be detected through rare elastic scatterings off nuclei in a sufficiently sensitive detector on Earth. The scatterings may however easily drown in a background of other effects picked up by the detector. To evade

this problem, one exploits the fact that the strength of the WIMP wind should display a seasonal variation with a well-defined period and phase. In June, the velocity of the Earth around the Sun is added to the velocity of the Sun around the Milky Way, it is giving maximal WIMP flux on Earth, whereas in December these two velocities act in the opposite directions, which is giving minimal WIMP flux. Because of this effect, the events induced by WIMPs should show an annular modulation [9].

1.3.3 MACHO

The MACHOs (Massive Astrophysical Compact Halo Objects) are large astrophysical objects (which for some reason do not emit much light) with masses substantially larger than those of WIMPs. Although the acronym was originally proposed with baryonic objects like failed stars in mind, many nonbaryonic candidates can in fact behave as MACHOs [4].

The MACHO populations that can be probed through microlensing effects are not necessarily subject to constraints on the baryonic mass fraction of the Universe, and can in principle constitute all of the DM. Certain kinds of MACHOs could furthermore have a sufficiently small interaction with the baryonic content of the Universe to effectively behave as CDM.

1.4 Implications for detection

For WIMPs X to have the observed relic density, they must annihilate to other particles. Assuming that these other particles are SM particles, the necessity of $XX \to SMSM$ interactions suggests three promising strategies for DM detection:

1. Indirect detection: if DM annihilated in the early Universe, it must also annihilate now through $XX \to SMSM$, and the annihilation products may be detected. The energetic electrons and positrons produced by WIMP annihilation interact with the CMB photons and up-scatter them to higher frequencies producing a peculiar SZ effect with specific spectral and spatial features [6].

2. Direct detection: DM can scatter of normal matter through $XSM \to XSM$ interactions, depositing energy that may be observed in sensitive, low background detectors. The elastic scattering of a DM particle off a target medium induces energy, for the case of the WIMP an energy transfer to nuclei, which can be observed through three different signals, depending on the detector

technology in use. These can be the production of heat (phonons in a crystal), an excitation of the target nucleus which de-excites releasing scintillation photons or by the direct ionization of the target atom [7].

3. Particle colliders: DM may be produced at particle colliders through $SMSM \rightarrow XX$. Such events are undetectable, but are typically accompanied by related production mechanisms, such as $SMSM \rightarrow XX + "SM"$, where $SM"$ denotes one or more standard model particles. These events are observ-able and provide signatures of DM at colliders.

1.5 Dark matter candidates

1. NEUTRALINOS

   The gauge hierarchy problem is most elegantly solved by supersymmetry [7]. In super symmetric extensions of the SM, every SM particle has a new, as yet undiscov-ered partner particle, which has the same quantum numbers and gauge interactions, but differs in spin by $\frac{1}{2}$. Not surprisingly, the doubling of the SM particle spectrum has many implications for cosmology. For DM, it is natural to begin by listing all the new particles that are electrically neutral. For technical reasons, supersymmet-ric models require two Higgs bosons . The neutral supersymmetric particles are then

   - Spin $\frac{3}{2}$ Fermions = Gravitino G
   - Spin $\frac{1}{2}$ Fermions = B, W, H_u, H_d Neutralinos = x_1, x_2, x_3, x_4
   - Spin 0 scalars = sneutrinos ν_e, ν_μ, ν_τ,

   As indicated, the neutral spin $\frac{1}{2}$ fermions mix to form four mass eigenstates, the neutralinos. The lightest of these, $x = x_1$ is a WIMP DM candidate. [4]

   The sneutrinos are not good DM candidates, as both their annihilation and scatter-ing cross sections are large, and so they are under abundant or excluded by null results from direct detection experiments for all masses near m_{weak}. The gravitino is not a WIMP, but it is a viable and fascinating DM candidate.

2. KALUZA-KLEIN dark matter

   The simplest universal exstra dimension (UED) models preserve a discrete parity known as KK-parity, which implies that the lightest KK particle (LKP) is stable and a possible DM candidate .The lightest KK particle (LKP) is typically B^1, the level 1 partner of the hypercharge gauge boson.

3. OTHERS

   Neutralinos are the prototypical WIMP, and KK DM provides an instructive exam-ple of WIMPs that differ in important aspects from neutralinos. In the recent years leading up to the start of particle collider, there has been a proliferation of electro weak theories and an accompanying proliferation of WIMP candidates. These include branons in theories with large extra dimensions, T-odd particles in little Higgs theories , and excited states in theories with warped extra dimensions . As with all WIMPs, these are astrophysically equivalent, in that they are produced through thermal freeze out and are cold and collisionless, but their implications for direct detection, indirect detection, and particle colliders may differ significantly [6].

1.6 Direct detection

WIMP DM may be detected by its scattering of normal matter through processes $XSM \rightarrow XSM$. Given a typical WIMP mass of $m_x \sim 100GeV$ and WIMP velocity $v \sim 10^{-3}kms^{-1}$, the deposited recoil energy is at most $100keV$, requiring highly sensitive, low background detectors placed deep underground. Such detectors are insensitive to very strongly interacting DM, which would be stopped in the atmosphere or earth and would be undetectable underground. However, such DM would be seen by rocket and other space-borne experiments or would settle to the core of the Earth. We may concentrate on the weak cross section frontier probed by undergrou-nd detectors [16].

WIMP scattering may be through spin-independent couplings, such as interactions $XXqq$, or spin-dependent couplings, such as interactions $x\gamma^{\mu}\gamma^{5}xq\gamma_{\mu}\gamma^{5}q$, which reduce to spin-spin couplings S_xS_q in the non relativistic limit $\nu q \rightarrow lq$.

Inelastic scattering, in which DM is assumed to scatter through $XSM \rightarrow X_0SM$, where X_0 is another new particle that is nearly $100keV$ heavier than X, has been put forward as one solution. Spin-dependent scattering provides an independent method to search for DM.

Direct detection methods are presently evolving rapidly, use the feeble interaction between DM particles of the galactic halo and nuclei such as Germanium, Sodium, Iodine, Argon, or Xenon to infer the scattering cross section and a rough estimate of the mass of the DM particle.

1.7 Indirect detection

DM may therefore be detected indirectly; DM pair-annihilates somewhere, producing something, which is detected somehow. There are many indirect detection methods being pursued. The idea behind neutrino searches is the following: when WIMPs pass through the Sun or the Earth, they may scatter and be slowed below escape velocity. Once captured, they then settle to the center, where their densities and annihilation rates are greatly enhanced. Although most of their annihilation produ-cts are immediately absorbed, neutrinos are not. Some of the resulting neutrinos then travel to the surface of the Earth, where they may convert to charged leptons through $\nu q \rightarrow lq$, and the charged leptons may be detected [9].

The neutrino flux depends on the WIMP density, which is determined by the competing processes of capture and annihilation. If N is the number of WIMPs captured in the Earth or Sun, $N = C - AN^2$, where C is the capture rate and A is the total annihilation cross section times relative velocity per volume. The present WIMP annihilation rate is, then,

$$\Gamma_A = \frac{AN^2}{2} = Ctanh^2\left(\frac{\sqrt{CAt_o}}{2}\right) \tag{1.9}$$

Where $t \sim 4.5Gyr$ is the age of the solar system. For most WIMP models, a very large collecting body such as the Sun has reached equilibrium. The annihilation rate alone does not tell about how the neutrinos are produced. However, if one assumes, say, that WIMPs annihilate to bb' or W^+W^-, which then decay to neutrinos, as is true in many neutralino models, the neutrino signal is completely determined by the capture rate C, that is, the scattering cross section. In addition to neutrinos, there are many other particles that may be signals of DM annihilation. The most prominent recent example is the detection of positrons and electrons with energies between $10GeV$ and $1Tev$ [20].

$$\Omega_{CDM}h^2 = 0.112 \pm 0.0056, \tag{1.10}$$

In addition to neutrinos from the Sun and positrons from the galactic halo, there are several other promising indirect detection search strategies. Searches for antiprotons and anti-deuterons from WIMP annihilation in the galactic halo provide complementary searches, as they are sensitive to DM candidates that annihilate

primarily to quarks. In addition, searches for gamma rays by space-based experiments, the ground-based atmospheric Cherenkov telescopes are also promising.

The most striking gamma ray signal would be mono-energetic photons from $XX \to \gamma\gamma$, but since WIMPs cannot be charged, these processes are typically loop-induced or otherwise highly suppressed. More commonly, gamma rays are produced when WIMPs annihilate to other particles, which then radiate photons, leading to a smooth distribution of gamma ray energies. On the other hand, photons point back to their source, providing a powerful diagnostic. Possible targets for gamma ray searches are the center of the Galaxy, where signal rates are high but backgrounds are also high and potentially hard to estimate, and dwarf galaxies, where signal rates are lower, but backgrounds are also expected to be low.

1.8 SuperWIMPS

In this section, we discuss superWIMPs, superweakly interacting massive particles, which have the desired relic density, but have interactions that are much weaker than WIMPS [4].

A , Production Mechanisms

(a) DECAYS

In the superWIMP framework, DM is produced in late decays: WIMPs freeze out as usual in the early Universe, but later decay to superWIMPs, which form the DM that exists today. Because superWIMPs are very weakly interacting, they have no impact on WIMP freeze out in the early Universe, and the WIMPs decouple, as usual, with a thermal relic density $\Omega_{WIMP} \sim \Omega_{DM}$. Assuming that each WIMP decay produces one superWIMP, the relic density of superWIMPs is:

$$\Omega_{SWIMP} = \frac{m_{SWIMP}}{m_{WIMP}} \Omega_{WIMP} \tag{1.11}$$

SuperWIMPs therefore inherit their relic density from WIMPs, and for $m_{SWIMP} \sim m_{WIMP}$, the WIMP miracle also implies that superWIMPs are produced in the desired amount to be much or all of DM. The superWIMP interacts only gravitationally, as is true of many well known candidates, the natural timescale for WIMPs decaying to superWIMP is

$$\frac{1}{G_N m_{weak}^3} \sim 10^3 - 10^7 s. \tag{1.12}$$

Because the WIMP is unstable and not the DM, it need not be neutral in this context, to preserve the naturalness of the superWIMP relic density, all that is required is $\Omega_{SWIMP} \sim \Omega_{DM}$.

(b) REHEATING

SuperWIMPs may also be produced after reheating, when the energy of the inflaton potential is transferred to SM and other particles. This creates a hot thermal bath, and, if the temperature is high enough, may be a significant source of superWIMPs.

B , particles

(a) WEAK-SCALE GRAVITINOS

The superWIMP scenario is realized in many particle physics models. The proto-typical superWIMP is the gravitino G. Gravitinos are the spin $\frac{3}{2}$ superpartners of gravitons, and they exist in all supersymmetric theories. The gravitino's mass is [1]

$$m_G = \frac{F}{\sqrt{3} M_*} \tag{1.13}$$

where F is the supersymmetry breaking scale squared and

$$M_* = (8\pi G_N)^{\frac{-1}{2}} \sim 2.4 \times 10^{18} GeV \tag{1.14}$$

is the reduced Planck mass. In the simplest supersymmetric models, where supersymmetry is transmitted to SM superpartners through gravitational interactions, the masses of SM superpartners are

$$m' \sim \frac{F}{M_0} \tag{1.15}$$

A solution to the gauge hierarchy problem requires

$$F \sim (10^{11} Gev)^2, \tag{1.16}$$

and so all superpartners and the gravitino have weak scale masses.

(b) Others

In addition to gravitinos, other well motivated examples of superWIMPs include axinos, the supersymmetric partners of axions, particles introduced to resolve the strong Charge Parity problem. Axions may also be cold DM candidate, and the possibility that both axions and axinos contribute to DM is one of the better motivated multi-component DM scenarios.

C , Indirect Detection

SuperWIMPs are so weakly interacting that they cannot be detected by direct searches, and their annihilation cross sections are so suppressed that their annihila-tion signal rates are completely negligible. However, if the decaying WIMP is charged, the superWIMP scenario implies long-lived charged particles, with striking implications for indirect detection [16]. One interesting possibility is that long-lived charged particl-es may be produced by ultra high energy cosmic rays, resulting in exotic signals in cosmic ray and cosmic neutrino experiments. As an example, in the gravitino superWIMP scenario with a stau, ultra high energy neutrinos may produce events with two long lived staus through $\nu q \to \tau q'$ followed by the decay $q' \to \ tau$

1.9 Hidden dark matter

Hidden DM is a DM that has no SM gauge interactions. Hidden dark matter has been explored for decade and leading to a large and diverse class of candidates. Most hidden DM candidates have no non-gravitational signals, which are most likely required if we are to identify DM [1].

1. THE WIMPLESS MIRACLE

   It is desirable for hidden DM to have naturally the correct relic density, just as in the case of WIMPs. One way to achieve this goal would be to duplicate the couplings and mass scales of the visible sector in the hidden sector so that the WIMP miracle is satisfied in the hidden sector. The thermal relic density of a stable particle with mass m_x annihilating through interactions with couplings g_x is [6]

$$\Omega_x \sim \langle \sigma_A v \rangle^{-1} \sim \frac{m_x^2}{g_x^4} \tag{1.17}$$

   The WIMP miracle is the fact that, for

   $m_x \sim m_{weak}$ and

$g_x \sim g_{weak} \sim 0.65$,

Ω_x is roughly $\Omega_{DM} \sim 0.23$

The above equation makes clear, however, that the thermal relic density fixes only one combination of the DM's mass and coupling, and other combi-nations of $(m_x; g_x)$ can also give the correct Ω_x. In the SM, g_x, g_{weak} is the only choice available, but in a general hidden sector, with its own matter content and gauge forces, other values of $(m_x; g_x)$ maybe realized. Such models generalize the WIMP miracle to the WIMPless miracle: darkmatter that naturally has the correct relic density, but does not necessarily have a weak scale mass or weak interactions .

2. particles

   The WIMPless miracle is naturally realized in particle physics frameworks that have several other motivations, the hidden sector superpartner masses are

$$m_x \sim \frac{g_x^2}{16\pi^2}\frac{F}{M_m} \tag{1.18}$$

   where g_x is the relevant hidden sector gauge coupling [5]. As a result

$$\frac{m_x}{g_x^2} \sim \frac{F}{16\pi^2 M_m} \tag{1.19}$$

   that is, $\frac{m_x}{g_x^2}$ is determined solely by the supersymmetry breaking sector. As this is exactly the combination of parameters that determines the thermal relic density is, the hidden sector automatically includes a DM candidate that has the desired thermal relic density, irrespective of its mass.

1.10 Sterile neutrinos

A light sterile neutrinos, is non interacting particle, which is one of DM candidate. We denote this neutrino, with mass m_s and mixing angle θ defined by

$$\nu_s = \nu_R cos\theta + \nu_L sin\theta \tag{1.20}$$

where ν_R or ν_L is a linear combination of righthanded (left-handed) gauge eigenstates [7].

A , Production Mechanisms

Sterile neutrinos may be produced in a number of ways. The relic density depends on the sterile neutrino mass and mixing angle, and all of the mechanisms require very small masses and mixing angles for sterile neutrinos to be viable DM candidates.

Sterile neutrinos may be produced by oscillations at temperatures $T \sim 100MeV$. Sterile neutrinos were never in thermal equilibrium, but the resulting distribution is near thermal. The results of numerical studies may be approximated by

$$\Omega_{\nu s} \sim 0.2 \left(\frac{sin^2 2\theta}{10^{-8}}\right) \left(\frac{M_s}{3kev}\right)^{1.8} \tag{1.21}$$

B , Indirect Detection

The dominant decay of sterile neutrinos is through $\nu_S \rightarrow \nu_L \nu'_L \nu_L$. However, sterile neutrinos may also decay through a loop-level process to a photon and an active neutrino with branching ratio [16]

$$\left(\frac{27\alpha}{8\pi}\right) = \frac{1}{128}. \tag{1.22}$$

The radiative decay width is

$$\Gamma(\nu_s \rightarrow \gamma\nu_\alpha) = \left(\frac{9\alpha}{2048\pi^4}\right) G_F^2 sin^2 2\theta m_s^5 \tag{1.23}$$

$$\Gamma(\nu_s \rightarrow \gamma\nu_\alpha) \sim \left(\frac{1}{1.5 \times 10^{32} s}\right) \left(\frac{sin^2 2\theta}{10^{-10}}\right) \left(\frac{m_s}{kev}\right)^5 \tag{1.24}$$

For the allowed sterile neutrino parameters, the sterile neutrino's lifetime is long, as required for it to be DM candidate.

1.11 Axions

Axions are motivated by the strong CP or charge parity problem. It is caused due to electric dipole moment of neutron to be 10^{10} times larger than the experimental upper bound. The axion solution follows from introducing a new pseudoscalar field with coupling [4]

$$L_a = \frac{-g_3^2}{32\pi^2} \frac{a}{f_a} \epsilon^{\mu\nu\rho\sigma} G^\alpha_{\mu\nu} G^\alpha_{\rho\sigma} \tag{1.25}$$

where f_a is a new mass scale, the axion decay constant. This term makes the coefficient of $\epsilon^{\mu\nu\rho\sigma}G^{\alpha}_{\mu\nu}G^{\alpha}_{\rho\sigma}$ dynamical. The vacuum energy depends on this coeficient, and it relaxes to a minimum where the neutron is very small and consistent with current bounds. As we will see, the allowed parameters for axions imply that they are extremely light and weakly interacting, providing yet another qualitatively different DM candidate.

A , Production Mechanisms

The axion's mass and interactions are determined by f_a up to model dependent constants. The axion's mass is

$$m_a = \frac{\sqrt{m_u m_d}}{m_u + m_d} m_\pi f_\pi \frac{1}{f_a} \tag{1.26}$$

$$m_a \sim 6\mu ev \left(\frac{10^{12} Gev}{f_a}\right) \tag{1.27}$$

where $m_u = 4MeV, m_d = 8MeV$, and $m_\pi = 135MeV$ are the up quark, down quark, and pion masses, and $f_\pi = 93MeV$ is the pion decay constant. Axions interact with gluons, through the term given above, and also with fermions. At loop-level, they also interact with photons through the coupling [1]

$$L_{a\gamma\gamma} = (-g_\gamma)\frac{\alpha}{\pi}\frac{a}{f_a} E \times B \equiv (-g_{a\gamma\gamma}) aE \times B; \tag{1.28}$$

where α is the fine-structure constant and g_γ is a model-dependent parameter. For two well known axions, g_γ is -0.97 and 0.36, respectively. The axion's mass is bounded by several independent constraints. The coupling of these equation implies that axions decay with lifetime

$$\tau(a \to \gamma\gamma) = \frac{64\pi}{g^2_{a\gamma\gamma} m_a^3} \tag{1.29}$$

$$\tau(a \to \gamma\gamma) \sim \left(\frac{8.8 \times 10^{23} s}{g_\gamma^2}\right)\left(\frac{ev}{m_a}\right)^5 \tag{1.30}$$

For axions to live long, $m_a \leq 20ev$. Axions may be produced in astrophysical bodies and then escape, leading to a new source of energy loss. There are several possible production mechanisms for axion DM. A prior the most straightforward is thermal production, as in the case of light gravitinos and sterile neutrinos. Unfortunately, Axions produced thermally would have a relic density of $\Omega_a^{th} \sim 0.22\left(\frac{m_a}{80ev}\right)$ and be hot DM [5].

B , Direct Detection

Axions may be detected directly by looking for their scattering with SM particles in the laboratory. For cosmological axions,the favored region of axion parameter space, in which axions may be all of the DM, may be taken to $1\mu ev < m_a < 100\mu eV$ [16].

CHAPTER 2

Methods of Analysing Dark Matter in the Galactic Cluster, Dark Halos and its Mathematical Model

2.1 Dark matter with Brane-f (R) gravity

The question of DM is presently one of the most pressing open problems in the study of universe. The galaxy rotation curves and mass discrepancy in a cluster of galaxies are two prominent observational evidence for the existence of DM. According to Newtonian gravity, galaxy rotation curves give the velocity of matter rotating in a spiral disk as a function of the distance from the center of a galaxy; it increases linearly within the galaxy and drops off as the square root of $\frac{1}{r}$ outside the galaxy [13].

$$v = \sqrt{\frac{GM}{r}} \tag{2.1}$$

v is the velocity of matter in the galaxy, M is its mass and r is the distance from the center of the galaxy. However, observations show that this is not the case and the velocity remains approximately constant. This provides for the possible existence of a new invisible matter distributed around galaxies which is known as DM .

The mass discrepancy of clusters as another evidence for the existence of DM and it can be understood when estimating the total mass of a cluster in two different ways; summing the individual member masses within the cluster leads to a total mass which we shall call M . Alternatively, the virial theorem applied to a cluster would yield an estimate of the cluster mass which we call M_v . As it turns out, M_v is nearly $20 - 30$ times greater than M and this difference is known as the virial mass discrepancy. The best way to deal with the above discrepancy, it seems, is to postulate DM [9].

There are several candidates for DM which can be categorized as baryonic or non-baryonic, or, as hot or cold according to their velocity at the time when galaxies were just starting to form. Thus to deal with the question of DM, modifications to

Einstein field equations have become a flourishing method in recent years. One such modification is the brane - f(R) gravity. Theories of gravity in which the Einstein Hilbert (EH) action is replaced with a generic function of R, the Ricci scalar, have been quite useful in dealing with the question of DM .

According to recent observations, the tangential velocity of matter moving around the center of a galaxy tends to a constant value as one moves away from the center of the galaxy. Such rotation curves have been studied in the context of brane world scenarios by using the concept of conformal symmetry. A vector field on a Riemannian manifold is called conformal Killing if it generates one parameter group of conformal transformation [15]

We present similar conclusions in a brane $f(R)$ model by using the idea of conformal Killing symmetry. In this regard, the spacetime is assumed to have, in addition to being static and spherically symmetric, a conformal symmetry. If the vector field ξ is the generator of such conformal symmetry, then the spacetime metric h is mapped conformally onto itself along the trajectories of ξ. [8]

$$L_{\xi} h_{\mu\nu} = \psi h_{\mu\nu}, \tag{2.2}$$

with L being the Lie derivative and ψ is the conformal factor.

2.2 Generalized Viral theorem in Brane-f(R) gravity

Cluster of galaxies are gravitationaly bound particles, to describe the statistical distribution of DM, we choose viral theorem in brane-f(R) Gravity. It is one of the method to study DM. In order to derive the virial theorem for galaxy clusters, it is necessary to introduce the brane - f(R) model we are interested in. We also need to know the Boltzmann equation governing the evolution of the distribution function in cluster of galaxies. By taking the cluster of galaxies as a system of identical and collisionless point particles, we utilize the relativistic Boltzmann equation together with the field equations to find the generalized virial theorem.

2.2.1 The Brane-f (R) gravity

In a brane f(R) model, the 5-dimensional bulk action is taken as [8]

$$S = \int d^5x\sqrt{-g}[f(R) + L_m], \tag{2.3}$$

where L_m is the matter lagrangian, g is the bulk metric and R is the bulk Ricci scalar . Variation of S with respect to the bulk metric g_{AB} yields

$$F(R)R_{AB} - 1/2g_{AB}f(R) + g_{AB}\Box F(R) - \nabla_A\nabla_B F(R) = \kappa_5^2 T_{AB}, \tag{2.4}$$

where$F(R) = df(R)/dR$. The effective Einstein field equa- tions in the bulk can be written as[8]

$$G_{AB} = R_{AB} - 1/2Rg_{AB} = T_{AB}^{tot} \tag{2.5}$$

where

$$T_{AB}^{tot} = \frac{1}{F(R)}[\kappa_5^2 T_{AB} - (\frac{1}{2}RF(R) - \frac{1}{2}F(R) + \Box F(R))g_{AB} + \nabla_A\nabla_B F(R)]. \tag{2.6}$$

Using the same procedure , the field equations on the brane are given by

$$G_{\mu\nu} = 8\pi G_N \tau_{\mu\nu} + \kappa_5^4\pi_{\mu\nu} + Q_{\mu\nu} - E_{\mu\nu}. \tag{2.7}$$

We note that

$$G_N = \frac{\kappa_5^4\lambda}{48\pi} \tag{2.8}$$

where λ is the brane tension, $\tau_{\mu\nu}$ is the energy momentum tensor on the brane and $\pi_{\mu\nu}$ is defined in terms of $\tau_{\mu\nu}$ as [8]

$$\pi_{\mu\nu} = \frac{-1}{4}\tau_{\mu\alpha}\tau_\nu^\alpha + \frac{1}{12}\tau\tau_{\mu\nu} + \frac{1}{8}h_{\mu\nu}\tau_{\alpha\beta}\tau^{\alpha\beta} - \frac{1}{24}h_{\mu\nu}\tau^2 \tag{2.9}$$

The electric part of the Weyl tensor is given by

$$E_{\mu\nu} = C_{BCD}^A n_A n^C h_\mu^B h_\nu^D, \tag{2.10}$$

where n_A is the unit vector normal to the 4-dimensional brane and $h_{AB} = g_{AB} - n_A n_B$ is the induced metric on the brane. Furthermore, we have

$$Q_{\mu\nu} = [\pi(R)h_{\mu\nu} + \frac{2}{3}\left(\frac{\nabla_A\nabla_B F(R)}{F(R)}\right)(h_\mu^A h_\nu^B + n^A n^B h_{\mu\nu})]_{y=0}, \tag{2.11}$$

and

$$\pi(R) = \frac{-4}{15}\frac{\Box F(R)}{F(R)} - \frac{1}{10}R\left(\frac{3}{2} + F(R)\right) + \frac{1}{4}f(R) - \frac{2}{5}\Box F(R), \tag{2.12}$$

where y is the extra dimension and the brane is located at $y = 0$. Now, if we define $Q_{\mu\nu} - E_{\mu\nu}$ as

$$Q_{\mu\nu} - E_{\mu\nu} = 8\pi G_N T_{\mu\nu}, \tag{2.13}$$

We obtain

$$G_{\mu\nu} = 8\pi G_N(\tau_{\mu\nu} + T_{\mu\nu}) + \kappa_5^4 \pi_{\mu\nu}, \tag{2.14}$$

where $T_{\mu\nu}$ may act as a new matter source on the brane induced by the $f(R)$ action in the bulk. It is convenient to represent this new matter by [15]

$$T_\mu^\mu = (\rho_x, P_x^r, P_x^\perp, P_x^\perp). \tag{2.15}$$

Let us now consider an isolated and spherically symmetric cluster described by the metric

$$ds^2 = -e^{\nu(r)}dt^2 + e^{\lambda(r)}dr^2 + r^2 d^2\theta + r^2 sin^2\theta d^2\varphi, \tag{2.16}$$

living on the brane. Suppose that the clusters are constructed from galaxies which are acting as identical and collisionless particles and described by the distribution function f_B . The energy momentum tensor may be written in terms of f_B as

$$\tau_{\mu\nu} = \int f_B m u_\mu u_\nu du, \tag{2.17}$$

where m is the cluster's member mass, u is the four velocity of the galaxy and

$$du = \frac{du_r du_\theta du_\varphi}{u_t} \tag{2.18}$$

is the invariant volume element of the velocity space [8]. The energy momentum tensor of the matter in a cluster is given by an effective density ρ_{eff} and an effective anisotropic pressure, with radial p_{eff}^r and tangential $p_{eff}^\perp$ components. In other words, we have

$$\rho_{eff} = \rho\langle u_t\rangle^2, \tag{2.19}$$

$$P_{eff}^r = \rho\langle u_r^2\rangle, \tag{2.20}$$

$$P_{eff}^\perp = \rho\langle u_\theta^2\rangle \tag{2.21}$$

$$P_{eff}^\perp = \rho\langle u_\varphi^2\rangle. \tag{2.22}$$

using

$$\tau_\mu^\nu = diag(-\rho_{eff}, P_{eff}^r, P_{eff}^\perp, P_{eff}^\perp) \tag{2.23}$$

and

$$u^{\mu}u_{\mu} = -1, \tag{2.24}$$

the field equations become [8]

$$e^{-\lambda}\left(\frac{-\lambda'}{r}+\frac{1}{r^2}\right)-\frac{1}{r^2} = 8\pi G_N\rho_{eff}+\frac{\kappa_5^4}{12}[-(\rho_{eff})^2+(p^r_{eff})^2-2(p^r_{eff})(p^{\perp}_{eff})+(p^{\perp}_{eff})^2]-8\pi G_N\rho_x \tag{2.25}$$

$$e^{-\lambda}\left(\frac{\nu'}{r}+\frac{1}{r^2}\right)-\frac{1}{r^2} = 8\pi G_N P^r_{eff}+\frac{\kappa_5^4}{12}[(\rho_{eff})^2+2(p^{\perp}_{eff})(\rho_{eff})-(p^r_{eff})^2+(p^{\perp}_{eff})^2]+8\pi G_N p^r_x, \tag{2.26}$$

and

$$e^{-\lambda}\left(\frac{\nu\prime}{2r}-\frac{\lambda\prime}{2r}-\frac{\nu\prime\lambda\prime}{4}+\frac{\nu\prime\prime}{2}+\frac{\nu\prime^2}{4}\right) = 8\pi G_N P^{\perp}_{eff}+\frac{k_5^4}{12}[(\rho_{eff})^2+(\rho_{eff})(p^r_{eff})(p^r_{eff})^2+8\pi G_N P^{\perp}_x. \tag{2.27}$$

We note that the $(\theta\theta)$ and $(\varphi\varphi)$ components of the field equations are similar. To derive the virial theorem, we need the Boltzmann equation which governs the evolution of the distribution function. By integrating this equation on the velocity space and using the gravitational field equations, the virial theorem can be obtained.

We consider the cluster as an isolated spherically symmetric system described by the above equation. Furthermore, we assume that the galaxies in the cluster behave like identical, collisionless point particles. The distribution function is denoted by f_B which obeys the general relativistic Boltzmann equation. The relativistic Boltzmann equation can be written as [21]

$$u^a e^{\mu}_a\frac{\partial f_B}{\partial x^{\mu}}+\gamma^i_{bc}u^b u^c\frac{\partial f_B}{\partial u^i} = 0 \tag{2.28}$$

where $f_B = f_B(x^{\mu}, u^a)$ is the distribution function and $\gamma^a_{bc} = e^a_{\mu,\nu}e^{\mu}_b e^{\nu}_c$ are the Ricci rotation coefficients .

We may assume that f_B depends only on the radial coordinate r. Thus, the relativistic Boltzmann equation [2] becomes

$$u_1\frac{\partial f_B}{\partial r}-\left(\frac{1}{2}u_0^2\frac{\partial\nu}{\partial r}-\frac{u_2^2+u_3^2}{r}\right)\frac{\partial f_B}{\partial u_1}-\frac{1}{r}u_1\left(u_2\frac{\partial f_B}{\partial u_2}+u_3\frac{\partial f_B}{\partial u_3}\right)-\frac{1}{r}u_3 e^{\frac{\lambda}{2}}cot\theta\left(u_2\frac{\partial f_B}{\partial u_3}-u_3\frac{\partial f_B}{\partial u_2}\right) = 0 \tag{2.29}$$

The term proportional to $cot\theta$ must be zero since the system is spherically symmertic. In velocity space f_B tends to zero, if the velocities tends to infinity. So we find

$$\frac{\partial}{\partial r}[\rho\langle u_r^2\rangle]+\frac{1}{2}\frac{\partial\nu}{\partial r}\rho[\langle u_t^2\rangle+\langle u_r^2\rangle]-\frac{1}{2}\rho[\langle u_\theta^2\rangle+\langle u_\varphi^2\rangle]+\frac{2}{r}\rho\langle u_r^2\rangle = 0 \tag{2.30}$$

Multiply the above equation by $4r^2$ and integrate over the cluster volume to obtain

$$\int_0^R \rho[\langle u_r^2\rangle + \langle u_\theta^2\rangle + \langle u_\varphi^2\rangle]4\pi r^2 dr - \frac{1}{2}\int_0^R \rho[\langle u_t^2\rangle + \langle u_r^2\rangle]\frac{\partial\nu}{\partial r}4\pi r^3 dr = 0 \tag{2.31}$$

where R is the radius of the cluster. Assuming that the galaxies in the cluster have velocities much smaller than the velocity of light, and using

$$\langle u^2\rangle = \langle u_t^2\rangle + \langle u_r^2\rangle + \langle u_\theta^2\rangle + \langle u_\varphi^2\rangle = 1, \tag{2.32}$$

we obtain a useful equation by summing all none zero components of the field equation

$$e^{-\lambda}(\frac{2\nu'}{r} - \frac{\nu'\lambda'}{2} + \nu'' + \frac{\nu'^2}{2}) = 8\pi G_N\rho + 8\pi G_N\rho'_x \tag{2.33}$$

where $\rho'_x = (\rho_x + p_x^r + 2p_x^\perp)$

it is a pure geometric term acting as a new matter source on the brane.We assume that ν' and λ' are slowly varying and are small and their product can be neglected, and $e^{-\lambda} = 1$ inside the cluster. We then have [8]

$$\frac{1}{2r^2}\frac{\partial}{\partial r}\left(r^2\frac{\partial\nu}{\partial r}\right) = 4\pi G_N\rho + 4\pi G_N\rho'_x \tag{2.34}$$

On the other hand, using the above assumptions, one may write the equation as

$$2K - \frac{1}{2}\int_0^R 4\pi r^3\rho\frac{\partial\nu}{\partial r}dr = 0 \tag{2.35}$$

where

$$K = \int_0^R 2\pi\rho[\langle u_r^2\rangle + \langle u_\theta^2\rangle + \langle u_\varphi^2\rangle]r^2 dr \tag{2.36}$$

is the total kinetic energy of the galaxies [8]. Multiplying the above equation by r^2 and integrating yields

$$G_N M(r) = \frac{1}{2}r^2\frac{\partial\nu}{\partial r} - G_N M_x(r) \tag{2.37}$$

where we have used

$$M = \int_0^R dM(r) = \int_0^R 4\pi\rho r^2 dr \tag{2.38}$$

as the baryonic mass. We have also defined

$$M_X = \int_0^R 4\pi\rho_x' r^2 dr \tag{2.39}$$

as the geometric mass of the system. Now consider the following definitions

$$\Omega = -\int_0^R \frac{G_N M(r)}{r} dM(r), \tag{2.40}$$

$$\Omega_x = \int_0^R \frac{G_N M_x(r)}{r} dM(r) \tag{2.41}$$

after multiplying the above equation by $\frac{dM(r)}{r}$ and rearrange it, we get

$$\Omega = \Omega_x - \frac{1}{2}\int_0^R 4\pi r^3 \rho \frac{\partial \nu}{\partial r} dr \tag{2.42}$$

where Ω is the gravitational potential energy of the system. Finally, the equation leads to the generalized virial theorem

$$2K + \Omega - \Omega_x = 0. \tag{2.43}$$

Alternatively, the above equation can be written in the form

$$2K - G_N \int_0^R \frac{M(r)dM}{r} - G_N \int_0^R \frac{M_x(r)}{r} dM = 0 \tag{2.44}$$

Now let us introduce the radii R_v andR_x

$$R_v = \frac{M^2}{\int_0^R \frac{M(r)}{r} dM(r)} \tag{2.45}$$

$$R_x = \frac{M_x^2}{\int_0^R \frac{M(r)}{r} dM(r)} \tag{2.46}$$

The viral massM_v is defined as

$$2K = \frac{G_N M M_v}{R_v} \tag{2.47}$$

when we substitute on the above equation, it leads to

$$\frac{M_v}{M} = 1 + \frac{M_x^2 R_v}{M^2 R_x} \tag{2.48}$$

From observation, the relation $\frac{M_v}{M} > 3$ holds true for most of the galactic clusters. Therefore one can easily approximate the last equation

$$\frac{M_v}{M} = \frac{M_x^2 R_v}{M^2 R_x} \tag{2.49}$$

Now one may note that some geometric terms appearing in the Einstein field equations above could effectively play a role in the gravitational energy. These geometric terms may be attributed to a geometric mass at the galactic or extra galactic levels and may be interpreted as DM. On the other hand, DM is the main contribution of mass in clusters [19]. It means that the contribut-ion of the baryonic mass is negligible in comparison with DM. The total mass of the cluster can then be estimated as

$$M_{tot} = M_x. \tag{2.50}$$

We also know that the virial mass is mainly determined by the geometric mass. It means that the geometric mass could be a potential candidate for the virial mass discrepancy in clusters. As a result, we conclude that

$$M_x = M_V = M_{tot}. \tag{2.51}$$

Therefore it can be written as

$$M_v = M\frac{R_v}{R_x} \tag{2.52}$$

In astrophysics [9], the virial mass is the mass of a gravitationally bound astrophysical system, assuming the virial theorem applies. In the context of galaxy formation and DM halos, the virial mass is defined as the mass enclosed within the virial radius r_{vir} of a gravitationally bound system, a radius within which the system obeys the virial theorem. This shows that the virial mass is proportional to baryonic mass and the proportionality constant has geometrical origins. We conclude that DM is the main contribution of mass in galactic cluster. So the existence of DM, related to its mass was described with viral theorm in Brane f(R) gravity model. This model assured that, in galactic cluster large amount of mass is contributed from DM.

2.3 Detecting of dark matter by gravitational lensing

A gravitational lens is a distribution of matter between a distant light source and an observer, that is capable of bending the light from the source as the light travels towards the observer. If the (light) source, the massive lensing object, and the observer lie in a straight line, the original light source will appear as a ring around the massive lensing object. If there is any misalignment, the observer will see an arc segment instead [13].

More commonly, where the lensing mass is complex (such as a galaxy group or cluster) and does not cause a spherical distortion of space time, the source will resemble partial arcs scattered around the lens. The observer may then see multiple distorted images of the same source; the number and shape of these depending upon the relative positions of the source, lens, and observer, and the shape of the gravitational well of the lensing object. There are three types of lensing [10]

1. Strong gravitational lensing is a gravitational lensing effect that is strong enough to produce multiple images, arcs, or even Einstein rings. Generally, the strong lensing effect requires the projected lens mass density greater than the critical density. For point-like background sources, there will be multiple images; for extended background emissions, there can be arcs or rings.

2. Weak gravitational lensing is thus an intrinsically statistical measurement, but it provides a way to measure the masses of astronomical objects without requiring assumptions about their composition or dynamical state. It is used, where the distortions of background sources are much smaller and can only be detected by analyzing large numbers of sources in a statistical way to find coherent distortions of only a few percent [10].

   The lensing shows up statistically as a preferred stretching of the background objects perpendicular to the direction to the centre of the lens. By measuring the shapes and orientations of large numbers of distant galaxies, their orientations can be averaged to measure the shear of the lensing field in any region. This, in turn, can be used to reconstruct the mass distribution in the area: in particular, the background distribution of DM can be reconstructed. Since galaxies are intrinsically elliptical and the weak gravitational lensing signal is small, a very large number of galaxies must be used in these surveys.

3. Gravitational microlensing is an astronomical phenomenon due to the gravitational lens effect. It can be used to detect objects that range from the mass of a planet to the mass of a star, regardless of the light they emit. Typically, astronomers can only detect bright objects that emit much light (stars) or large objects that block background light (clouds of gas and dust). These objects make up only a minor portion of the mass of a galaxy [18].

Microlensing allows the study of objects that emit little or no light. Since microlensing observations do not rely on radiation received from the lens object, this effect therefore allows astronomers to study massive objects no matter how faint. It is thus an ideal technique to study the galactic population of such faint or dark objects as brown dwarfs, red dwarfs, planets, white dwarfs, neutron stars, black holes, and massive compact halo objects. Moreover, the microlensing effect is wavelength-independent, allowing use of distant source objects that emit any kind of electromagnetic radiation.

Microlensing by an isolated object can be detected by astronomers. Since then, microlensing has been to constrain the nature of the DM. When light is coming from a distant bright source such as a star, it has been formed a partial arc around DM, these mechanism helped us to study the property and nature of DM. we can analyze the distortion and the spherical arc of the light, which helped to specify and predict the stastical distribution and amount of DM in the galctic cluster and its subhalos.

2.4 The Sunyaev Zeldovich (SZ) effect(s)

2.4.1 Normal Compton scattering

A photon of initial wavelength λ and energy $h\nu$ deflected off a stationary free electron by an angle θ exhibits a wavelength gain and energy loss after scattering (S), in the form of energy and momentum conservation. Compton scattering is one of the major physical processes that couples matter and radiation[11].

$$\lambda_s - \lambda = \lambda_c(1 - cos\theta) \tag{2.53}$$

$$h\nu_s = \frac{h\nu}{1 + \lambda_c(\nu/c)(1 - cos\theta)} \tag{2.54}$$

$$\lambda_c = \frac{h}{m_e c} = 2.43 \times 10^{-12} m \tag{2.55}$$

λ_c is compton wavelength.

2.4.2 Inverse Compton scattering

The Inverse Compton Scattering process consists of low energy photons that upscatter in energy on high energy electrons and positrons. Photons gain energy from electro-ns. Photons are moved from less to more energetic regions of black-body spectrum. In the present case, the high energy $e^{\pm}$ are produced by DM annihilations in any given point of the galaxy, with a density determined by the DM distribution profile and with a spectrum dictated by the primary annihilation products [11].

The inverse Compton scattering of electrons or positrons from DM annihila-tion or decay with the interstellar and extragalactic radiation fields produces gamma rays. The bath of low energy target photons consists of three main contributions:

1. the starlight originating from stars of the galactic disk (at optical wavelengths),
2. the infrared radiation produced by the absorption and subsequent re-emission of such starlight by the galactic dust and finally
3. the ubiquitous microwave photons of the CMB.

Relativistic electrons and positrons from DM annihilation scatter the ambi-ent CMB photons, producing a spectral peak between the soft to hard X-ray bands depending on the mass of the DM particles. The inverse effect, i.e. the scattered photon gains energy, can be calculated from the normal Compton effect via appropriate Lorentz transformations in and out of the electrons system of reference.

2.4.3 SZ effect

The Sunyaev Zeldovich Effect(SZE) was theoretically predicted by Sunyaev and Zeldovich. SZE is the distortion of the blackbody Cosmic Back ground Radiation-(CMB) spectrum owing to Inverse Compton scattering of the CMB photons with the energetic Intra cluster medium(ICM) electrons. Photons of the (cold) CMB can be up-scattered to higher energies via Inverse Compton Scattering when passing through the hot electrons of the ICM [12].

The Sunyaev Zeldovich effect, which arises from the scattering of electrons in clusters of galaxies on the cosmic microwave background radiation field is perhaps

the most important astrophysical example to study the DM content in the cluster of galaxy. The effect provides a cosmological probe, it has been used to measure the properties of gas and DM in clusters of galaxies and its sub halos, and it can also be used as a means of measuring the motions of clusters of galaxies and hence studying the evolution of structure in the Universe.

On average the CMB photons gain energy in this process due to the thermal SZE, the CMB appears hotter when looking in the direction of massive galaxy clusters. The tSZE offers new observational possibilities for galaxy cluster surveys and cosmological applications.

The surface brightness of the SZE signal is in principle redshift independent for resolved systems, which could make it a powerful tool for detecting galaxy clusters at high red shift. The passage of radiation through an electron population with significant energy content will produce a distortion of the radiation's spectrum. The effect of thermal electrons on the CMBR is addressed in terms of the three likely sites for such a distortion to occur:

1. the atmospheres of clusters of galaxies
2. the ionized content of the Universe as a whole, and
3. ionized gas close to us.

using the plank distribtion and the plank black body formula [12]

$$I_\nu(T) = \frac{2h\nu^3}{c^2}\frac{1}{e^{\frac{h\nu}{k_bT}} - 1} \tag{2.56}$$

The final formula for thermal SZ effect is[12]

$$\frac{\partial I_\nu}{I_\nu} = \frac{\partial n}{n} = (-y)\left(\frac{xe^x}{e^x - 1}\right)[4 - xcoth(\frac{x}{2})]x = \left(\frac{\hbar w}{k_bT_{rad}}\right) \tag{2.57}$$

where n is phase space occupation number, k_b is boltzmann constant.

2.5 Non interacting mathematical model of dark matter

If DM is a boson with spin unity, it dose not couple with fermions. Indeed, it is the vector meson S first proposed by Weyl on the basis of scale invariance. Since

the S meson is a boson, it may form a condensate boson, which is translucent to light. The gravitational field generated by this condensate bends the light beam that passes through it. Therefore, a translucent condensate, if it exists, acts like a lens to light.

Indeed, S is a kind of DM coupling with neither quarks and leptons, nor any of the gauge mesons. Indeed, in our theory, the only interactions S has are those with the graviton and scalar mesons, the only candidate of which at the moment is the Higgs meson [21].

Let $g_{\mu\nu}$ be the metric tensor. Then the distance between two neighboring space-time points is

$$ds^2 = g_{\mu\nu}dx^\mu dx^\nu. \tag{2.58}$$

Let us change the metric tensor from

$g_{\mu\nu}$ to $g'_{\mu\nu}$,

where

$$g'_{\mu\nu} = \Lambda^2 g_{\mu\nu}, \tag{2.59}$$

with Λ a constant. Then we have

$$ds'^2 = \Lambda^2 ds^2, \tag{2.60}$$

$$ds'^2 = g'_{\mu\nu}dx^\mu dx^\nu. \tag{2.61}$$

Thus, with the transformation equation, the numerical value of the distance between two given points is changed by a constant multiple. Since $g^{\mu\nu}$ is the inverse of $g_{\mu\nu}$, then we have

$$g'^{\mu\nu} = \Lambda^{-2} g^{\mu\nu}, \tag{2.62}$$

We also have from above transformation equation that [21]

$$(-detg')^{\frac{1}{2}} = \Lambda^4(-detg)^{\frac{1}{2}}, \tag{2.63}$$

where $detg$ is the determinant of the matrix $g_{\mu\nu}$. The tetra ε^a_μ satisfies

$$\eta_{ab}\varepsilon^a_\mu\varepsilon^b_\nu = g_{\mu\nu}, \tag{2.64}$$

where η_{ab} is the metric tensor in the Minkowski space. Thus the tetrad transforms like

$$\varepsilon_{\mu}^{\prime a} = \Lambda \varepsilon_{\mu}^{a} \tag{2.65}$$

From the above equation, we have

$$\varepsilon^{\prime a\mu} = \Lambda^{-1} \varepsilon^{a\mu} \tag{2.66}$$

$$\varepsilon^{a\mu} = g^{\mu\nu} \varepsilon_{\nu}^{a} \tag{2.67}$$

From Hilbert action principle

$$\int d^4x (-detg)^{\frac{1}{2}} L \tag{2.68}$$

where L is the Lagrangian density. The action is invariant under global scale transformations provided that [15]

$$L' = \Lambda^{-4} L \tag{2.69}$$

Consider the Lagrangian of a massless scalar field ϕ with a ϕ coupling which is given by

$$\frac{1}{2} g^{\mu\nu} \partial_{\mu}\phi \partial_{\nu}\phi - \lambda \phi^4, \tag{2.70}$$

where λ is the quartic coupling constant. The Lagrangian which satisfies the above equation provided that

$$\phi' = \Lambda^{-1} \phi \tag{2.71}$$

Next consider the Lagrangian density of the electromagnetic field A_{μ}

$$\frac{-1}{4} g^{\mu\rho} g^{\nu\sigma} F_{\mu\nu} F_{\rho\sigma} \tag{2.72}$$

where

$$F_{\mu\nu} = \partial_{\mu} A_{\nu} - \partial_{\nu} A_{\mu} \tag{2.73}$$

This Lagrangian density satisfies the above equation and provided that

$$A'_\mu = A_\mu. \tag{2.74}$$

The Yang Mills theory is also invariant under global scale transformations. This is because

$$F^a_{\mu\nu} = \partial_\mu W^a_\nu - \partial_\nu W^a_\mu - g f^{abc} W^b_\mu W^c_\nu \tag{2.75}$$

is invariant under global scale transformations provided that [21]

$$W'^a_\mu = W^a_\mu, \tag{2.76}$$

where W_μ is the Yang Mills gauge meson, g is a dimensionless coupling constant, and f^{abc} is the structure constant of the gauge group. Thus gauge mesons do not couple with S. Neither does a fermion. Thus after a certain calculation we conclude that the fermion does not couple with S which is the expected DM particle. So DM particles are non interacting which is bound by gravity and the exchanging force is graviton [19].

Nuclei are formed as protons and neutrons attract one another with strong interactions. Solids or liquids are formed as electrons and nuclei have the electromagnetic interac-tion. Since the S mesons of DM have gravitational interactions, they cannot form the kinds of matter we expected. Thus the S particles mostly move freely in space, with nothing to reveal their existence other than through the gravitational field they generate. On the other hand, unlike fermions and baryons, S is a boson and does not satisfy the exclusion principle. As a result, there is no limit to how many S particles may occupy the same spatial point at the same time. Therefore, when the density of such particles become sufficiently high, they can be bound together by gravitational forces [2].

Thus it may be possible to form a condesation yet different from those of ordinary matters. In particular, they are translucent to light and can be heavy. The gravitational field generated from such a condensate bends the light that passes through it. Thus a translucent condensate, if it exists, acts like a lens that bends light. The above explanation tell us, DM consists of non interacting large particles and they are non baryonic particles which can be described by super symmetric model and it consists of boson particles. One of the candidate is weakly interacting massive

paricles WIMPS.

2.6 Big Bang nucleosynthesis

Since the 1950s [5], the Big Bang scenario has held the leading position as the most successful model for the origin and evolution of the Universe. The Universe started out extremely hot and dense some 14.1 Gyr ago. Early on, there where no galaxies, no stars and no planets. The Universe was instead filled by a gas of sub atomic particles at an extremely high density. As space expanded, the energy density dropped and the cosmic plasma cooled. After about 3 minutes, the Universe had cooled sufficiently to allow synthesis of the light elements H, He, Li and Be. This epoch of Big Bang nucleosynthesis (BBNS), after which most of the baryons were in the form of H and He, ended when the proton gas become sufficiently diluted by the expansion of the Universe to prevent further reactions. At around 240 000 years after the Big Bang, the Universe had reached a sufficiently low temperature $(\sim 4000K)$ to allow protons and electrons to form neutral hydrogen (the so-called epoch of recombination). Shortly thereafter, at around 350 000 years after the Big Bang, hydrogen fell out of equilibrium with the photons, and the Universe became transparent to radiation. The Black body radiation originating from this cosmic plasma is still permeating the Universe in the form of the Cosmic Microwave Background Radiation (CMBR) which can be observed at $T = 2.73K$ with radio telescopes .

2.7 Density contribution of DM in the universe

Due to the expansion of space, electromagnetic radiation emitted in the distant Universe is redshifted on its path towards us, so that the observed wavelength of light, $\lambda_{obs},$ is larger than the wavelength at which it was emitted, λ_{emit} . The longer the light path through the expanding cosmos, the larger is the amount of redshift induced. Redshift can therefore be used to determine the distances to astronomical objects. The redshift, z, is defined to be [13]

$$z = (\frac{\lambda_{obs}}{\lambda_{emit}}) - 1 \tag{2.77}$$

$$z = \left(\frac{a_{obs}}{a_{emit}}\right) - 1 \tag{2.78}$$

where a is the cosmic scale factor (which can be set to $a_{obs} = 1$ at the present time).

High redshift therefore simultaneously refers to the early and distant Universe, whereas low redshift indicates the local and recent Universe.

By adopting the cosmological principle, which assumes the universe to be spatially homogeneous and isotropic on large scales, a number of equations governing the evolution of the Universe can be derived from Einstein's theory of general relativity. The resulting Friedmann equations, which form the basis of most contemporary cosmology, can be written:[7]

$$\frac{\dot{a}^2 + kc^2}{a^2} = \frac{8\pi G\rho_{tot}}{3} \tag{2.79}$$

$$\frac{2\ddot{a}}{a} + \frac{\dot{a}^2 + kc^2}{a^2} = -\frac{8\pi G p_{tot}}{c^2} \tag{2.80}$$

where ρ_{tot} represents the total mass density of the Universe, p_{tot} the total pressure, and k the curvature parameter which determines the overall cosmic geometry. From these two, the Raychaudhuri (or acceleration) equation can be drived as

$$\frac{2\ddot{a}}{a} = -\frac{8\pi G}{3c^2}\Sigma(\rho_i c^2 + 3p_i) \tag{2.81}$$

in which ρ_i and p_i represent the densities and pressures of the different components which contribute to the total density of the Universe. The total density of the Universe is simply the sum over its i components:

$$\rho_{tot} = \Sigma\rho_i. \tag{2.82}$$

It is however more convenient to describe the different contributions to the current total density of the Universe with the use of the Ω parameter:

$$\Omega_i = \frac{\rho_i}{\rho_c} \tag{2.83}$$

where the critical density ρ_c is the density required to make the Universe spatially flat $(k = 0)$. The critical density at the present time is given by[9]

$$\rho_c = \frac{3H_0^2}{8\pi G} \tag{2.84}$$

where H_0 represents the current value of the Hubble parameter H =$\frac{\dot{a}}{a}$. This critical density corresponds to

$\rho_c = 9.2 \times 10^{-27} kgm^{-3}$

for the currently favoured

$H_0 = 70 kms^{-1}Mpc^{-1}$.

The most important contributions to the density ρ_{tot} of the Universe are often assumed be [20]

$$\rho_{tot} = \rho_{DM} + \rho_{rad} + \rho_{\Lambda} \tag{2.85}$$

where ρ_{DM} represents the density contribution from nonrelativistic matter or DM and ρ_{rad} the corresponding contribution from relativistic matter or radiation. The last term, ρ_{Λ} , describes the density contribution from a so-called cosmological constant Λ. Current measurements of the cosmological parameters are consistent with a spatially flat $(k = 0)$ Universe with

$$\Omega_{tot} = \Omega_{DM} + \Omega_{\Lambda} \tag{2.86}$$

it implies negligible contributions from radiation and relativistic matter, where $\Omega_{DM} = 0.3$ and $\Omega_{\Lambda} = 0.7$.

CHAPTER 3

Statistical Studies of Dark Matter Dominated Subhalos

3.1 Statistical studies of dark matter

Observations of the large scale distribution of galaxies and simulations of the clustering of DM have produced a reasonably coherent picture, in which the CDM is distributed in a foam, soap-bubble and spiderweb like structure of voids, filaments and walls with characteristic sizes of $\sim 100Mpc$. In high density regions, almost spherical structures known as DM halos are expected to form. Inside these, baryons collapse through dissipation to form luminous galaxies of stars and gas. In the CDM picture, the dark halos merge in a hierarchical fashion into larger and larger halos [14].

Today, the Universe is filled with dark halos with masses ranging from dwarf galaxy ($\sim 10^6 M_0$) to giant galaxy cluster ($\sim 10^{15} M_0$) scale. Inside each of the more massive dark halos, smaller subhalos reside, so that each cluster mass halo is filled with a large number of galaxy mass halos, and each galaxy-mass halo with halos of dwarf galaxy mass.

The case for the existence of dark halos around galaxies is nowadays rather strong. Galactic disks would quickly turn into giant bars without the stabilizing influence of a massive, spheroidal component such as a dark halo. The weak, statistical image distortions imposed on distant objects in large galaxy catalogues by the matter distribution in foreground objects (so called weak gravitational lensing) also confirm the DM distribution to be reasonably consistent with CDM halos. The density and dynamics of the Milky Way are dominated by a thick DM disk out to a radius of $35kpc$ from the centre [20].

We live in a universe that is energetically dominated by DM and dark energy (DE). For DM at least we have a well motivated theoretical framework, in which

it is comprised of fundamental particles predicted to arise in extensions of the standard model of particle physics like supersymmetry. We estimate the expected distribution of displacements between the DM and gas cores in simulated clusters. We use the MareNostrum Universe, one of the largest non radiative, ΛCDM cosmological simulations.

In bullet cluster, the difference between DM and gas in $2D$ projection by mass, is equal or larger than , $10^{14}h^{-1}M_0$. The $2D$ displacement distribution is roughly the same between redshifts $0 < z < 0.5$, when multiplied by a factor of $(1+z)^{\frac{-1}{2}}$. The matter and energy density of the Universe Ω is often described in terms of a relative density [1]

$$\Omega = \frac{\rho}{\rho_c}, \tag{3.1}$$

$$\rho_c = \frac{3H_0^2}{8\pi G_N} \tag{3.2}$$

$$\rho_c = 1.88 \times 10^{-29} h^2 g/cm^3 \tag{3.3}$$

$$\rho_c = 1.1 \times 10^{-5} h^2 GeV/cm^3, \tag{3.4}$$

ρ_c is the critical density to close the Universe, H_0 is the Hubble constant,

$$h = H_0/(100 kmsec^{-1} Mpc^{-1}), \tag{3.5}$$

and G_N is the Newton's gravitational constant. At the same time the universe is also expanding and it is describe by Hubble equation

$$v = H_0 d \tag{3.6}$$

$H_0 = 70 kmsec^{-1} Mpc^{-1}$ is Hubble constant, v is the speed and d is the distance in Mpc.

Galaxy clusters have no well defined physical edge, and we must adopt some convention for determining a boundary for the systems and their enclosed mass. The common approach is to define the boundary of a cluster as a sphere enclosing an average matter density equal to some chosen reference overdensity, Δ_{ref} , times some reference background density, ρ_{ref}. The mass of the cluster is then [1]

$$M_{\Delta_{ref}} = \frac{4\pi}{3}\Delta_{ref}\rho_{ref}(z)r^3_{\Delta_{ref}} \tag{3.7}$$

where $r_{\Delta_{ref}}$ is the cluster radius. The two common choices of the background density ρ_{ref} are the critical density, $\rho_c(z)$, and the mean matter density, $\rho_m(z)$,

$$\rho_c(z) = \frac{3H_0^2}{8\pi G}(\Omega_m(1+z)^3 + \Omega_\Lambda) \tag{3.8}$$

$$\rho_m(z) = \frac{3H_0^2}{8\pi G}\Omega_m(1+z)^3 \tag{3.9}$$

in the standard ΛCDM spatially flat cosmological model. The reference overdensity, Δ_{ref} , is usually chosen to be a number close to $18\pi^2 = 180$, correspond to the virial overdensity under the spherical collapse model in the Einstein-deSitter universe where $\Omega_m = 1 - \Omega_\Lambda = 1$. It is assumed that the density parameter is due to matter only. Compare this to the the currently accepted cosmological model for the Universe, ΛCDM model, where $\Omega_m = 0.3$ and $\Omega_\Lambda = 0.7$. In this case, $\Delta_c \approx 100$. Nevertheless it is typically assumed that $\Delta_c = 200$ for the purpose of using a common definition, and this is denoted as r_{200} for the virial radius and M_{200} for the virial mass. Using this convention, the mean density is given by

$$\rho(< r_{200}) = 200\rho_c(t) = 200\frac{3H^2(t)}{8\pi G}. \tag{3.10}$$

Other conventions for the overdensity constant include $\Delta_c = 500$, depending on the type of analysis being done, in which case the virial radius and virial mass is signified by the relevant subscript. In the more realistic flat ΛCDM universe, the virial overdensity is not constant and varies with redshift. Conventionally $\rho_c(z)$ has been adopted as the reference background density for the cluster mass definition: $\rho_{ref} = \rho_c(z)$ with $\Delta_{ref} = \Delta_c = 500$ [13].

The standard model of structure formation describes the Universe as a three component fluid (DM (DM), gas and radiation) plus a cosmological constant. The interaction between DM and baryons is only through gravitational forces, one can expect a decoupling between the components, when the collisional nature of baryons becomes important. From the observational point of view, the decoupling is evident in collisions of high mass clusters, observed, for the first time, in the Bullet Cluster. For this object, a combined analysis of strong and weak gravitational lensing and X-ray observations gives a displacement of around $200kpc$ between the density peak of the gaseous and DM components in the cluster halos.

The standard explanation for this decoupling between DM and gas, is the collision between clusters of galaxies. For example, in the case of a collision between two clusters of comparable mass, the DM halos and galaxies go through each other without falling apart from two body trajectories while the intra-cluster medium, dominated by pressure effects, is stripped out of the DM halos. The velocity of the expected collision could be inferred observationally from the temperature of the bow shock that is usually present in the collisions[14]. But the velocity of the encounter between DM structures has large statistical and systematic uncertainties. Statistical study of this decoupling would become possible through weak lensing and galaxy number counts as a proxy for DM distribution and the X-ray emission as a tracer of the gas component.

The statistical distribution of the density field is investigated by means of a counts-in-cells method in a low density cold DM (CDM) simulated universe. To measure the clustering of objects (galaxies, haloes, clusters, etc.) on large scales corresponds to the distribution of count of objects in cells $p_v(N)$, defined as the probability of finding N objects in a randomly placed cell of volume V . In practice, rather than estimating the whole count-in-cells distribution (Probability Distribution Function), the first moments of the distribution function, like the variance, and the skewness, are estimated. There are four model of distributions, namely the negative binomial distribution, the lognormal distribution, the Edge-worth series and the skewed lognormal distribution. These are tested to fit the calculated distribution function, and it is shown that only the skewed lognormal distribution of second and third order can describe the evolution of the statistical distribution perfectly well from the initially Gaussian regime to the present stage [17].

The structures in the Universe originate from tiny density fluctuations emerging from a primordial Gaussian field after an early inflationary period. Gravitational instability in an homogeneous expanding Universe dominated by Cold DM, indeed gives rise to the rich variety of structures seen today by hierarchical clustering.

3.2 Microhalo density profiles

DM haloes provide the potential well in which galaxies subsequently form. As a consequence the structural parameters of disk galaxies (size and rotation velocity) are tightly coupled with those of their hosting DM halo, such as concentration and spin. The structural properties of DM haloes are dependent on halo mass, that means if the mass haloes are higher, their concetrations are less. In order

to quantify the detectability of microhalos and the survival probability as galactic subhalos, one needs to know the form of their density profiles and their typical concentrations. The concentration is defined as $c_{200} = r_{200}/r_s$, where r_{200} is the radius enclosing 200 times the critical density of the Universe.

3.2.1 Dark matter density profile: smooth component

For the smooth component of the DM density profile, we consider two models: one is the NFW (Navarro, Frenk and white) profile , and the other is the Einasto profile with a central core. The NFW profile is given by [5]

$$\rho(r) = \frac{\rho_s}{(\frac{r}{r_s})(\frac{r}{r_s}+1)^2} \tag{3.11}$$

where ρ_s and r_s are the scale density and scale radius, respectively. The mass M_{vir} and redshift z are given inputs, and the virial radius r_{vir} is obtained by solving

$$M_{vir} = 4\pi r_{vir}^3 \Delta_{vir}(z)\rho_c(z)/3, \tag{3.12}$$

where $\rho_c(z)$ is the critical density of the universe.

$$\Delta_{vir}(z) = 18\pi^2 + 82d - 39d^2 \tag{3.13}$$

$$d = \Omega_m(1+z)^3/[\Omega_m(1+z)^3 + \Omega_\Lambda] - 1 \tag{3.14}$$

The scale radius r_s is then defined as $r_s = r_{vir}/c_{vir}$, where c_{vir} is the concentration parameter.

$$c_{vir}(M_{vir}, z) = \frac{7.85}{(1+z)^{0.71}} \left(\frac{M_{vir}}{2\times 10^{12} h^{-1} M_0}\right)^{-0.081} \tag{3.15}$$

By taking volume integral of $\rho(r)$ up to the virial radius r_{vir} and then equating it to M_{vir}, we obtain

$$\rho_s = \frac{M_{vir}}{4\pi r_s^3}[ln(1+c_{vir}) - \frac{c_{vir}}{1+c_{vir}}]^{-1} \tag{3.16}$$

The Einasto profile, on the other hand, has the following functional form [20]

$$\rho(r) = \rho_e exp[-d_n|(\frac{r}{r_e})^{\frac{1}{n}} - 1|] \tag{3.17}$$

$$d_n = 3n - \frac{1}{3} + \frac{0.0079}{n} \tag{3.18}$$

where n and r_e are the free parameters. The normalization ρ_e is obtained such that the total mass with in r_{vir} agrees with the measured equation. so

$$\rho_e = \left(\frac{M_{vir} d_n^{3n}}{4\pi r_e^3 n e^{d_n}} \right) \Gamma(3n, d_n [\frac{r_{vir}}{r_e}]^{\frac{1}{n}})^{-1} \tag{3.19}$$

where $\Gamma_{(a,x)}$ is the lower incomplete gamma function.

3.2.2 Dark matter contraction due to baryon dissipation

The DM density profile is modified as a result of baryon dissipation. A so-called DM contraction model is based on the conservation of the angular momentum[3]

$$M_i(r_i')r_i = [M_{dm,i}(r_i') + M_{b,f}(r_f)]r_f \tag{3.20}$$

where $M(r)$ is the mass enclosed within the radius r, subscripts dm and b are for DM and baryons, respectively, and subscripts i and f represent quantities before and after the contraction, respectively. The masses inferred from, e.g. gravitational lensing or X-ray observations are the total mass, and therefore one must assume underlying distributions of both baryons and DM inorder to infer $M_{dm,i}$.

We simply assume that DM and baryons trace each other exactly; namely, $\rho_{dm,i}(r) = (1 - fb)\rho_i(r)$ and $M_{dm,i}(r) = (1 - fb)M_i(r)$, where f_b is the baryon fraction at virial radius. For the final profiles of baryons, on the other hand, we use the observed distribution of stars and gas, giving the baryon mass distribution to be

$$M_{b,f}(r) \sim M_i(r) + M_{gas}(r) \tag{3.21}$$

The DM mass profile after the contraction is then obtained by

$$M_{dm,f}(r_f) = M_{dm,i}(r_i(r_f)). \tag{3.22}$$

If particle orbits can be approximated to be circular and if the contraction happens adiabatically, then we simply have $r' = r$. This is a so-called standard adiabatic contraction model, based on hydro dynamical simulations, presented the above modified formula and pointed out that corrections to the adiabatic contraction model can be accommodated by modifying a relation between r' and r as

$$\frac{r'}{r_{vir}} = 0.85 \left(\frac{r}{r_{vir}} \right)^{0.8} \tag{3.23}$$

This was further investigated and found that the relation is generalized as

$$\frac{r'}{r_0} = A_0 \left(\frac{r}{r_\circ}\right)^w \tag{3.24}$$

well represents the simulation results, where $r_0 = 0.03 r_{vir}$, and w ranges from 0.5 to 1.3, if A_0 is fixed to 1.6. Here we adopt $w = 0.8$ as a canonical value for this parameter, but also consider the cases of $w = 0.6$ and 1. In addition, we adopt $A_0 = 1$ and $w = 1$, the standard adiabatic contraction, as an extreme case scenario.

3.3 Simulation

Cosmological N body simulations have been widely used to study the nonlinear structure formation of the universe and have been an important tool for a better understanding of our universe. Using the results of high-resolution simulations of small-scale structures, we can study the fine structures of galactic halos, the distribution of subhalos, their structures are depend on the nature of DM. The analysis of DM uses mainly the Marenostrum Universe cosmological simulation [13].

The simulation works on the evolution of halos in a $30Mpc$ cubic box using 2048^3 particles. The mass of particles are $1.28 \times 10^5 M_0$. The resolution reaches down to ultra faint dwarf-galaxy-sized halos ($\sim 10^7 M_0$). We focus on the halo mass function with the mass down to $10^7 M_0$, the structures of most massive halos, and statistics of the internal properties of dwarf-galaxy-sized halos.

This non-radiative simulation was run using the evolution of gas and DM from $z = 40$ to $z = 0$ in a comoving cube of $500h^{-1}Mpc$ on a side. The cosmology used corresponds to the spatially flat concordance model with the following parameters: the total mass density $\Omega_m = 0.255$, the baryon density $\Omega_b = 0.045$, the cosmological constant $\Omega_\Lambda = 0.7$, the Hubble parameter $h = 0.7$, the slope of the initial power spectrum $n = 1$ and the normalization $\sigma_8 = 0.9$.

The number of particles used for each of the DM and gas component was 1024^3, resulting in a mass of $8.3 \times 10^9 h^{-1} M_0$ for the DM particles and $1.5 \times 10^9 h^{-1} M_0$ for the gas particles with r_{200}. The spatial force resolution was set to an equivalent Plummer gravitational softening of $15h^{-1}kpc$ commoving.

Given the highly non-linear nature of hierarchical structure formation, the substructure of DM haloes is best studied using high-resolution N-body simulations. These

studies not only used different simulation codes, different cosmologies, different numerical resolutions, and different simulation volumes, but also different subhalo finders. Different subhalo finders have been used, the following two characteristics of a subhalo [18]

1. it is a self-bound, overdense region inside its hosthalo, and
2. it was its own host halo before it merged into its current host.

Most halo finders only use the instantaneous particle positions and velocities to identify subhaloes. Examples of such halo finders are SUBFIND, Bound Den-sity Maximum (BDM), Amiga Halo Finder (AHF), and Voronoi Bound Zoner. Others, such as six-dimensional friends of friends (6DFOF), Hierarchical Structure Finder and ROCKSTAR, identify (sub)haloes using the full 6D phase-space informa-tion. More quantitatively, SUBFIND was only able to recover 50 per cent of the subhalo mass when its centre is located at half the virial radius from the centre of its host. At $r < r_{vir}/10,$ neither subhalo finder could recover more than 40 per cent of the actual subhalo mass. We use subhalo mass functions (SHMFs) and subhalo catalogues from a variety of numerical simulations that are publicaly available, and that have been obtained using different subhalo finders, to compare SHMFs, focusing on the massive end.

3.3.1 Separation measurement algorithm

These analysis is to obtain the distribution of displacements between the dominant density peaks of the DM and gas components of each selected cluster in the simulation. We describe first the algorithm used on a set of hierarchical friend of friends (FOF) catalogs. Then, we describe briefly a different and more complex algorithm of structure detection, which, nevertheless, gives the same statistical results than the hierarchical FOF.

3.3.2 FOF based algorithm

The simulations with the hierarchical friend of friends (FOF) algorithm used for the DM and gas particles, separately. The basic FOF groups were identified using a linking length of $b = 0.17$ times the mean inter particle separation both for the gas and the DM distribution. The substructures inside the FOF groups are defined as FOF objects constructed with shorter linking lengths $b_n = \frac{b}{2^n}(n = 1, 2, 3)$. We name these catalogs FOF_n^{DM} and FOF_n^{gas} with $(n = 0, 1, 2, 3)$ for the DM and gas

components [14].

The main objective is to measure the physical separation between the dominant gas clump in the cluster, with respect to its predominant DM structure. We find the separation based on the FOF catalogs. The main advantage of the FOF algorithm is that it can be easily applied to the subsets of DM particles and gas particles and identifies gas clumps even if they don't have a pronounced density peak. Moreover, the set of linking lengths in the hierarchical FOF allows to find objects at different over densities.

We describe the clusters as the objects detected in the $DMFOF_0$ catalog. FOF_0 provides objects with about virial overdensity, whereas FOF_i provides substructures with about 2^{3i} higher densities. In all cases we find that the clusters exhibit a massive dominant gas clump and various DM clumps. In both DM and gas catalogs we define the dominant clump position in the following way. We identify first the center and radius of the cluster as given by the $DMFOF_0$ catalog. Next we find the most massive group in the FOF_1 catalog with its center inside the radius defined previously. The clump defines a new center and radius. Then iterate this procedure until we cannot find a new group in the following FOF_i catalog. The outputs of the algorithm are the mass and radius of the cluster defined from the $DMFOF_0$ catalog and the centers of mass of the dominant DM and gas clumps as well as their separation.

3.3.3 AHF based algorithm

As an example of a spherical over density halo finder we have used the Amiga Halo Finder (AHF) which identifies both halos and subhaloes. AHF locates local over densities in a adaptively smoothed grid as prospective halo centers.

The AHF algorithm proceeds by creating a hierarchy of grids. High refined grids are spanned in high density regions until a minimum number of particles per grid-cell is reached [14]. The algorithm includes a criterion to span a new mesh refinement, which is usually expressed as a density threshold. To find the positions of the gas and DM clumps, we run AHF over the gas and DM distribution separately. Thus the positions can be associated to the regions where the corresponding mesh refinement reached its highest level.

For Amiga Halo Finder, we have to follow the following algorithm [9]

- Finding prospective halo centers.

- Collecting particles possibly bound to the center.
- Removing unbound particles.
- Calculating halo properties.
- Organizing the adaptive mesh refinement (AMR) hierarchy into a tree structure and classify it into host halos and subhalo.

AMR grids are isodensity contours, which help to encompass particles.

AHF algorithm use the following mechanism to idetify halos and subhalos

1. collect all particles inside unambiguous isodensity contour
2. consider particles inside half distance sphere, too
3. determine halo edge and Δ_{vir} virial overdensity threshold is calculated inside AHF which is depend on redshift. Remove outliers and remove unbound particles.
4. iteratively remove unbound particles,

   assume spherical symmetry

   $$\rho = \rho(r) \tag{3.25}$$

   solve poisson's equation [18]

   $$\Delta\varphi = 4\pi G\rho \tag{3.26}$$

   first integration

   $$\frac{1}{r^2}\frac{d}{dr}(r^2\frac{d\varphi}{dr}) = 4\pi G\rho. \tag{3.27}$$

   but

   $$\varphi = r^2\frac{d\varphi}{dr} \tag{3.28}$$

   $$\frac{1}{r^2}\frac{d\varphi}{dr} = 4\pi G\rho, \tag{3.29}$$

   $$\frac{d\varphi}{dr} = 4\pi G\rho r^2 \tag{3.30}$$

   $$\varphi(r) - \varphi(0) = 4\pi G\int_0^r \rho r'^2 dr' \tag{3.31}$$

   where

   $$\varphi(0) = [r^2\frac{d\varphi}{dr}]_{r=0} = 0 \tag{3.32}$$

   $$M(< r) = 4\pi\int_0^r \rho r'^2 dr' \tag{3.33}$$

$$\varphi(r) = GM(< r) \tag{3.34}$$

assume spherical symmetry

$$\rho = \rho(r) \tag{3.35}$$

solve Newton's force law

$$\frac{d\varphi}{dr} = \frac{GM(< r)}{r^2} \tag{3.36}$$

second integration

$$\varphi(r) = G\int_0^r \frac{M(< r')}{r'^2}dr' + \varphi(0) \tag{3.37}$$

it is unbound if

$$\nu > \nu_{esc} = \sqrt{2|\varphi|} \tag{3.38}$$

using potential normalisation at infinity, we deduce

$$\varphi(\infty) = G\int_0^\infty \frac{M(r')}{r'^2}dr' + \varphi(0) \tag{3.39}$$

$$\varphi(\infty) = G\int_0^{R_{vir}} \frac{M(< r')}{r'^2}dr' + GM_{vir}\int_{R_{vir}}^\infty \frac{1}{r'^2}dr' + \varphi(0) \tag{3.40}$$

$$\varphi(\infty) = G\int_0^{R_{vir}} \frac{M(< r')}{r'^2}dr' + G\frac{M_{vir}}{R_{vir}} + \varphi(0) \tag{3.41}$$

but

$$\varphi(r) = G\int_0^r \frac{M(< r')}{r'^2}dr' - \varphi_0 \tag{3.42}$$

with

$$\varphi_0 = G\left(\frac{M_{vir}}{R_{vir}} + \int_0^{R_{vir}} \frac{M(< r')}{r'^2}dr'\right) \tag{3.43}$$

then order particles with respect to distance

$$\int_0^r \frac{M(< r')}{r'^2}dr' = \frac{m_1}{r_1^2}r_1 + \frac{m_1+m_2}{r_2^2}|r_2 - r_1| + \frac{m_1+m_2+m_3}{r_3^2}|r_3 - r_2| + ... \tag{3.44}$$

From these equation

(a) obtain initial set of particles and determineM_{vir} and R_{vir}

(b) calculate

$$\varphi_\circ = G\left(\frac{M_{vir}}{R_{vir}} + \int_0^{R_{vir}} \frac{M(< r)}{r'^2}dr'\right) \tag{3.45}$$

(c) while looping over all particles check unbound if

$$v_i > v_{esc}(r_i) = \sqrt{2|\varphi(r_i)|} \tag{3.46}$$

(d) bound particles define a new set of initial particles M_{vir} and R_{vir}. Start from 2 again and repeat until no further unbound particles.

(e) Then determine halo properties including subhalos which are contributing to the integral properties of their hosts [18].

3.3.4 Cummulative probability distributions

When we check the dynamical state of two different samples of the clusters at redshift zero. The first sample included those with large displacements $(> 200kpc)$ and the second sample comprises all clusters with low displacement $(< 10kpc)$ between gas and DM. The third sample is between $10kpc$ and $200kpc$. We found that, indeed all clusters with large displacements come from plunging substructures [9]. Moreover, those clusters which show the most extreme displacements also present a rich variety of merging configurations, with triple DM cores in some cases. On the other hand, in all the cases of clusters with low displacments, the dominant gas blob has a unique DM core associated to it, with practically zero relative velocity between them [14].

From the simulations, we know the three dimensional positions of the dominant DM and gas clumps. In order to compare our results with observations, we use 2D projections of the 3D displacements into 10 different randomly selected directions. We quantify the result using the cumulative distribution of the projected 2D displacements. Using the 10 different 2D displacement distributions and bin logarithmically the data in distance and find the mean value and dispersion for the corresponding cumulative distribution.

3.3.5 Scaling with cluster mass

We present the cumulative distribution of projected 2D displacements in the$MN-1024$ simulation. We bin the selected clusters in mass, and calculate the distribution for the 2D physical displacements. The mass bins are selected in such a way as to have a similar number of clusters in each bin at $z = 0.5$. We find that, at $z = 0$, the fraction of clusters with small physical separations, $(200kpc)$ increases with cluster mass. In constrast, at redshifts $z = 0.3$ and $z = 0.5$, we cannot assert that this trend with halo mass exists at all. In any case, in the range of the Bullets

clusters displacements, the distributions of different mass bins are less than 1% apart for all the redshifts. The fraction of simulated clusters with a displacement equal or larger than the observed ones is always between 1% and 2%. The lowest value corresponds to the less massive clusters at $z = 0$ and the highest value is associated with clusters at high redshifts $z = 0.5$ [17].

3.3.6 Scaling with redshift

All clusters more massive than $10^{14}h^{-1}M_0$ were taken into account for the construction of these distributions. When we consider the rescaled variable $\frac{d}{\sqrt{1+z}}$, where z corresponds to the redshift, the cummulative distributions turn out to be the same for all the redshifts analyzed [14]. A Schechter-like function turns out to be a good fit to the numerical results. In terms of the redshift scaled variable :

$$d_z = \frac{d}{\sqrt{1+z}} \tag{3.47}$$

$$p_{2d} = p_0 \left(\frac{d_z}{d_\star}\right)^\alpha exp\left(\frac{-d_z}{d_\star}\right) \tag{3.48}$$

with parameters $P_0 = 0.04, d_\star = 200kpc$ and $\alpha = -1.0$, fit very well in the range $100 < d_z/kpc < 500$.

3.4 Subhalo finders

Hierarchical structure formation in acold DM (ΛCDM) cosmology gives rise to DM haloes with abundant substructure in the form of self-bound clumps of matter. These subhaloes are the remnants of DM haloes that have been accreted by their host halo over cosmic time, and that have survived tidal destruction. The subhalo abundance shows large halo to halo variations and depends on the concentration parameter. Halos with larger concentrations have a smaller number of subhalos. This means that the number of subhalos should increase as the halo mass increases since the concentration decreases.

DM subhaloes host satellite galaxies, boost the DM annihilation signal, cause tidal heating of stellar streams and discs, and are responsible for time-delays and flux-ratio anomalies in gravitational lensing. The subhalo mass functions (SHMFs) presented below have been obtained using four different subhalo finders: SUBFIND, BDM, ROCKSTAR and SURV [20].

3.4.1 Bound-density-maximum

The bound-density-maximum (BDM) algorithm, identifies both host haloes (also called distinct haloes) and subhaloes . It locates density maxima in the particle distribution and uses an iterative scheme to remove unbound particles. If two haloes are

- separated by less than one virial radius,
- have masses that differ by less than a factor of 1.5, and
- have a relative velocity less than 0.15 of the rms velocity of DM particles inside the haloes,

BDM removes the smaller halo and keeps only the larger one.

3.4.2 SUBFIND

The SUBFIND algorithm is similar to BDM in that, it identifies substructures within a host halo by searching for overdense regions using a local density estimate, obtained by kernel interpolation over the nearest neighbours. It identifies substructure candidates as regions bounded by an isodensity surface that traverses a saddle point of the density field and uses an iterative unbinding procedure to ensure that these potential substructures are physically bound.

3.4.3 ROCKSTAR

ROCKSTAR (Robust Overdensity Calculation using K Space Topologically Adaptive Refinement) is a phase-space halo finder designed to maximize halo consistency across time-steps. It starts by splitting the particle distribution in large groups using a standard 3D FOF algorithm, but with a relatively large linking length of $b = 0.28$. Each of these 3D FOF groups is then analysed separately.

ROCKSTAR adaptively picks a linking length in 6D phase space such that 70 per cent of the group's particles are linked together in one or more subgroups. This process is repeated for each subgroup, hierarchically, until a predetermined minimum number of particles (standard is 10) remain at the deepest level of the hierarchy. When determining the host-subhalo hierarchy, ROCKSTAR uses the 6D phase-space distances between the various halo seeds, combined with results from halo catalogues at earlier outputs to assure consistency across outputs [14].

3.4.4 SURV

The subhalo finder SURV identifies subhaloes within the virial radius of a final host halo by following their progenitors from the time they were first accreted by the host main progenitor. Hence, SURV differs from the methods discussed above, in that it uses prior information based on the host halos merger history to identify its subhaloes. In particular, subhaloes are identified as those subsets of particles that belonged to one and the same progenitor halo at its moment of accretion. For haloes that have undergone a recent major merger, unbinding is done using the gravitational potential of the combined system.

3.5 Analytical model

This model uses a simple semi analytical description for the average subhalo mass-loss rate to evolve the masses of DM subhaloes from the moment of accretion to $z = 0$. It also yields the maximum circular velocities, V_{max}, for both host haloes and subhaloes. For host haloes, V_{max} is computed assuming that the density distribution of DM haloes follow an NFW profile (Navarro, Frenk & White 1997), so

$$V_{max} = 0.465 v_{vir} \sqrt{\frac{c}{ln(1+c) - \frac{c}{1+c}}} \tag{3.49}$$

where c is the halo's concentration parameter, and

$$V_{vir} = 159.43 kms^{-1} \left(\frac{M}{10^{12} h^{-1} M_0} \right)^{\frac{1}{3}} [\frac{H(z)}{H_0}]^{\frac{1}{3}} [\frac{\Delta_{vir}(z)}{178}]^{\frac{1}{6}} \tag{3.50}$$

is the virial velocity of a DM halo of virial mass M at redshift z. Here $H(z)$ is the Hubble parameters, and $\Delta_{vir}(z)$ specifies the average density of a collapsed DM halo in units of the critical density, ρ_{crit} , and is well represented by the fitting function [19]

$$\Delta_{vir}(z) = 18\pi^2 - 82\Omega_\Lambda(z) - 39\Omega_\Lambda^2(z). \tag{3.51}$$

The halo concentration is strongly correlated with the halo's assembly history, the model that relates halo concentration to the time $t_{0.04}$ at which the main progenitor of a halo of mass M at time t first exceeds a mass of $0.04M$, according to the following equation

$$c(M,t) = 4.0[1 + (\frac{t}{3.75t_{0.04}})^{8.4}]^{\frac{1}{8}} \tag{3.52}$$

So the concentration and the mass of dark matter in sub halos can be easily analyzed with the observational data.

CHAPTER 4

Result and Discussion

White and Rees (1978) made a seminal proposal about the process of galaxy formation. They suggested that galaxy formation occurs in two different stages. At first they proposed that the dominant dark matter component of the universe collapses into small clumps at an early epoch and that these dark clumps continue clustering in a hierarchical way. This process leads to a self-similar distribution of bound masses, which correspond to what we usually call dark matter haloes. The second stage in the galaxy formation process corresponds then to the cooling and condensation of the baryonic mass trapped within the potential wells of the dark matter clumps. Since the processes of formation and clustering of dark matter haloes in a cosmic density field involves only gravity, it appears that the problem of spatial galaxy clustering can be well approximated by understanding the spatial clustering of dark matter haloes and the formation of galaxies in individual dark haloes. In this way the clustering of dark matter haloes is studied by means of the gravitational theory and the formation of individual galaxies in a halo is traced using realistic models of galaxy formation in dark halos [13].

The amount of dark matter can be calculated by gravitational lensing. When there is a large source of light such as light from a galaxy which is located behind a body of large mass, the mass of the body acts as a lens and bends the light coming from the source. Therefore, when we observe this system, we will observe multiple images of light around the mass. The greater the lensing effect caused by a body, the larger is its mass. Because we understand general relativity, we can work backwards and calculate how much mass should be there in the system in order to produce that image. This will give the total mass of the system and if you subtract the visible mass of the lens, you get the amount of dark matter in that system. Dark matter particles have a mass greater than 40 giga electron volts (GeV) , approximately 42 times the mass of a proton. The Planck mission had revealed that in our universe ordinary baryonic matter, dark matter and dark energy are

present in the ratio: 4.9%, 26.8% and 68.3% respectively [18].

From N body simulation of 1024^3 partices in a box , we use ROCKSTAR halo finder with FOF algorithm, to analyze mass to light ratio, dark matter fraction, stellar fraction, gas fraction, baryon fraction and the amount of stars in the halos and its sub halos which helps to describe the properties and structure of gas and dark matter in the cluster halos.

Using MareNostrum universe catalogue, there are 282 clusters, in which their center are located in three dimensional coordinate. We can determine dark matter halos around their center using ROCKSTAR halo finder. The minimum number of particles is 100, with in the radius of $30kpc$ and for comparison we also analyse more than 50 particles, with a radius of $15kpc$. We select five clusters randomly, their cluster number is 00001, 00142, 00280, 00281 and 00282. The first two clusters are larger mass clusters and the last three clusters have smaller mass.

We analyze the dark matter halos in each clusters with in the radius of $30kpc$ which contain more than 100 particles and a radius of $15kpc$, in which its minimum particle is more than 50. Based on this analyses, we described the properties of dark matter in each cluster using simulation code. We plotted a scattered graph using different parameters. Each dot in each graph represent dark matter subhalos with a mass of around $10^7 M_0$. We will describe the properties of dark matter with different parameters and analyze the following quantities:

1. Mass to light ratio

   Mass to light is the ratio of the total mass to a star mass in a certain cluster, when we divide total mass of the given cluster to the star mass in that cluster, we can determine mass to light ratio. We plotted the graph of mass to light ratio versus total mass. From the graph, we observe that, the concentration of the halos is high for smaller mass of a cluster. For the total mass between $1 \times 10^{10} M_0 h^{-1}$ and $10 \times 10^{10} M_0 h^{-1}$, the mass-to-light ratio is between 100 to 10 respectively. It is highly concentrated region of halos and subhalos, which are located in the smaller mass region of the cluster. It implies that the dark matter halos are more concentrated in the smaller mass region of the cluster. But when the mass is above $10 \times 10^{10} M_0 h^{-1}$ M/L ratio is exponentially decreasing as shown in Fig 4.1.

   On the other hand, we calculated the halo distribution of 282 clusters, we found that, the total number of subhalos are about 466621. From these data

we suggest that, a large part of these clusters are occupied by DM halos.

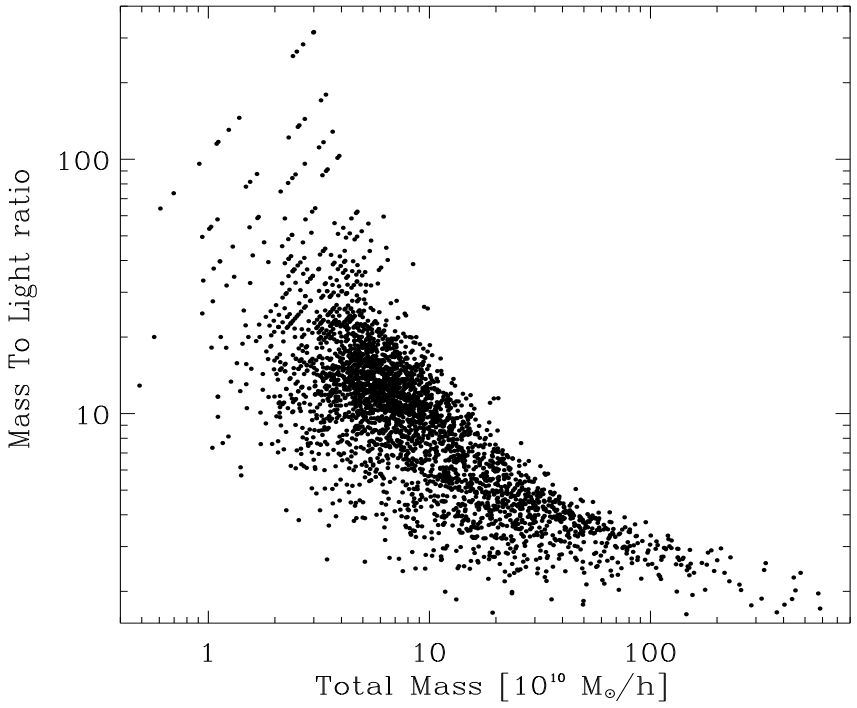

Figure 4.1: Mass to light ratio in the cluser with in 30 kpc radius

Mass to light ratio versus distance, in the ratio of r to r_{200} or Δr, will be shown in Fig 4.2. The viral radius r_{200} is a radius in which the density of the halos is 200 times the average density. When $\frac{r}{r_{200}}$ is between 0.1 and 2.5, the mass to light is between 1.1 and 100. It is the most dense region. The highest peak of mass to light ratio is located around $1 \times r_{200}$ and the cocentration of DM halos is also high at these radius. It is the radius in which the DM contain its relic density.

We will consider the graph of number of sub halos against $\frac{r}{r_{200}}$, in which its mass to light rario is more than 50 and 100 as shown in Fig 4.3. If M/L ratio is more than 50, the largest number of sub halos are located around 0.75 of r_{200}. But if M/L ratio is more than 100, the maxmimum peak is around 1.05 times r_{200}. If the number of subhalos increase, the amount of DM content will increase. So the DM content is high around the radius, $\Delta r = 0.75$. In both cases the number of subhalos are gradually decreasing above $\Delta r = 1.4$.

The statistical data of subhalos are:

(a) total counts above M/L of 1 is 132332

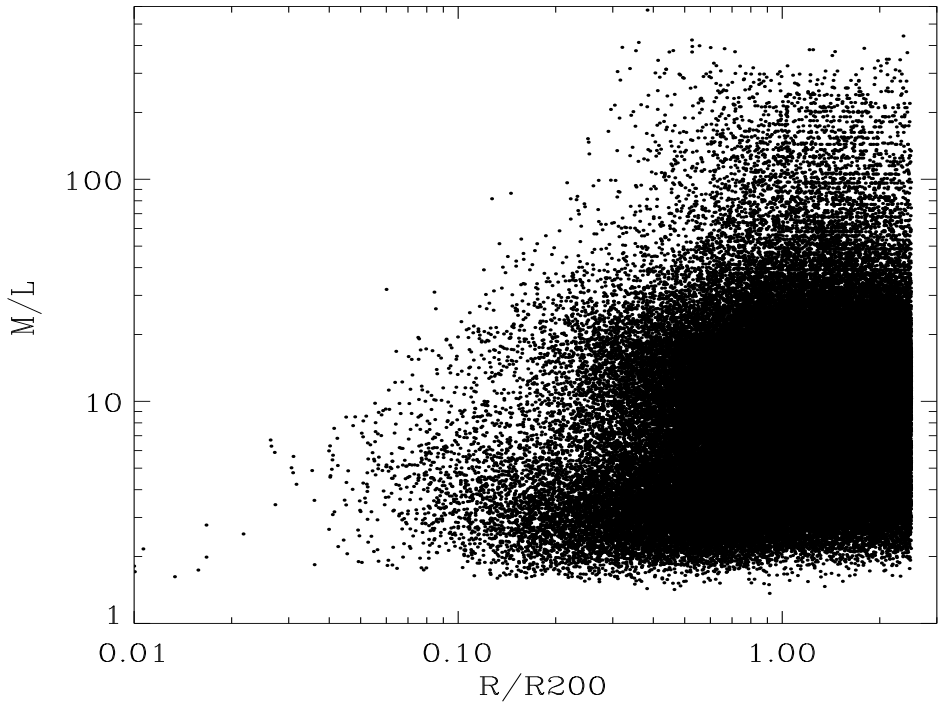

Figure 4.2: Mass to light versus distance

(b) total counts above M/L of 50 is 3131

(c) total counts above M/L of 100 is 1215.

When we compare these data to the total number of subhalos which is 466621, we found that about 28% of subhalos have mass to light ratio is more than 1. Based on these data, we can justify that the mass of DM is dominated in these cluster, which is directly related to the number of subhalos. The higher the number of subhalos indicate that more DM content are present in the cluster.

2. Dark matter fraction

DM fraction is determined by dividing the mass of DM to the total mass of the cluster. We select randomly five cluster from the catalogue and we plot DM fraction versus total mass of each cluster, using MareNostrum universe catalogue and ROCKSTAR halo finder simulation code within the radius of $30kpc$ and the minimum number of particle is 100. The DM fraction is about 80 to 90 percent in the range of $0.5 \times 10^{10} - 3 \times 10^{10} M_0/h$. The concentration of DM sub-haloes is high with in the range of 0.3×10^{10} to $10 \times 10^{10} M_0 h^{-1}$. In the region above $10 \times 10^{10} M_0/h$ the DM fraction is decreasing linearly. So the statistical distribution of DM halos are more for smaller mass cluster as

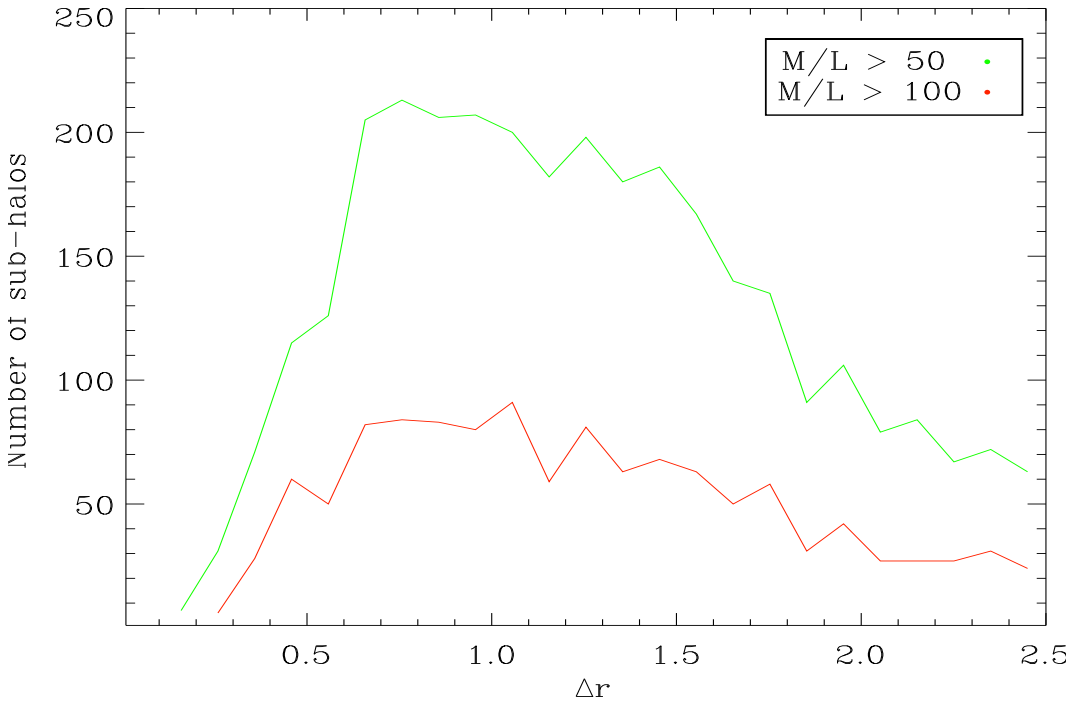

Figure 4.3: The number of subhalos versus Δr.

shown in Fig 4.4.

DM fraction for cluster 00001 is shown in Fig 4.5. From $0.5 \times 10^{10} - 2 \times 10^{10} M_0/h$, the DM fraction is high. The concentration of DM sub-halo is more for smaller mass cluster, in which its mass range is bettween $2 \times 10^{10} - 10 \times 10^{10} M_0/h$. Above $10 \times 10^{10} M_0/h$, the DM fraction is decreasing. We conclude that the DM fraction is related to the mass of cluster, in which its value is high in smaller cluster.

The main criterion in my thesis is to compare the DM fraction and mass to light ratio of the same cluster in different radius and different number of particles.

(a) DM fraction of the cluster 00281 with in the radius of 30 kpc and the minimum number of particle is 100, as shown in Fig 4.6. The concetration and the statistical distribution of DM is high in the range of mass $1 \times 10^{10} - 20 \times 10^{10} M_0/h$.

(b) DM fraction of the cluster 00281 with in the radius of 15 kpc and the minimum number of particle is 50, as shown in Fig 4.7. The statistical distribution DM content is high in the range of mass $0.5 \times 10^{10} - 10 \times$

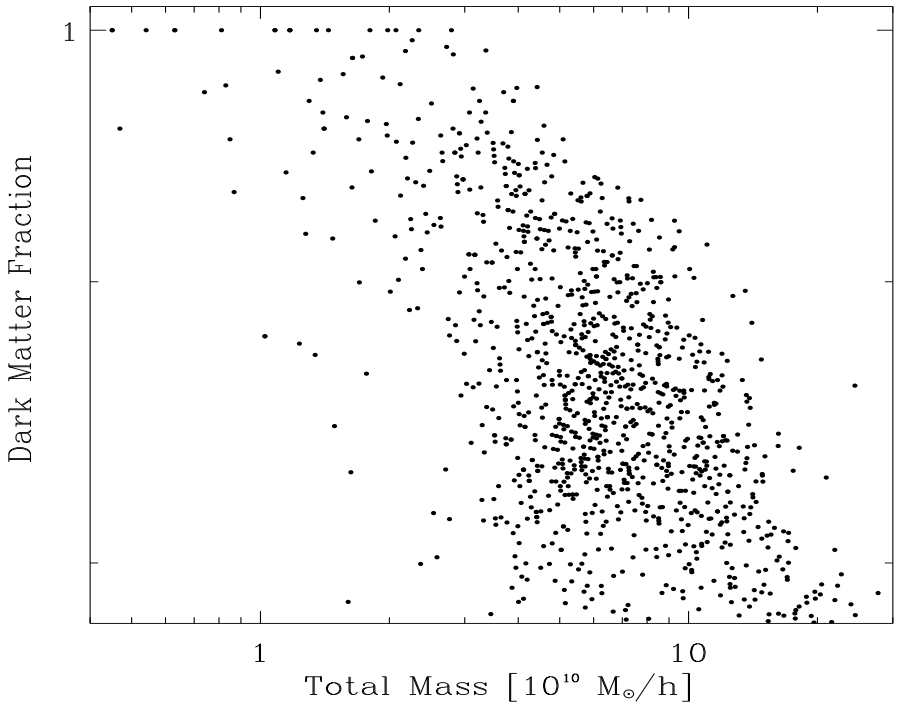

Figure 4.4: DM fraction versus total mass in the cluster of 00282 with in 30 kpc radius

$10^{10}M_0/h$.

(c) Mass to light ratio of the cluster 00281 with in the radius of 15 kpc, in which the minimum number of particle is 50, as shown in Fig 4.8.

Mass to light ratio is high in the range of $0.5 \times 10^{10} - 10 \times 10^{10}M_0/h$. Its concentration is decreasing exponentially above $10 \times 10^{10}M_0/h$.

When we compare the DM content of the same type of cluster 00281, with the differnt radius and different number of particles, we found that, the probablity of finding DM sub halos is high between the mass of $1 \times 10^{10} - 10 \times 10^{10}M_0$, in both radius, but it is highly concentrated on $15kpc$ radius, as we compare it with $30kpc$. Eventhough the concentration of DM halo is high for smaller mass with in the cluster in both cases, the radius and the minimum number of particle present in the cluser is also affect the statistical distribution of DM halos in the cluster.

3. Stellar fraction

Stellar mass is the sum of the mass of gas and stars. We can calculate stellar fraction, when we divide stellar mass to the total mass. From the graphical point of view of simulated clusters, which is listed below, we can justify that,

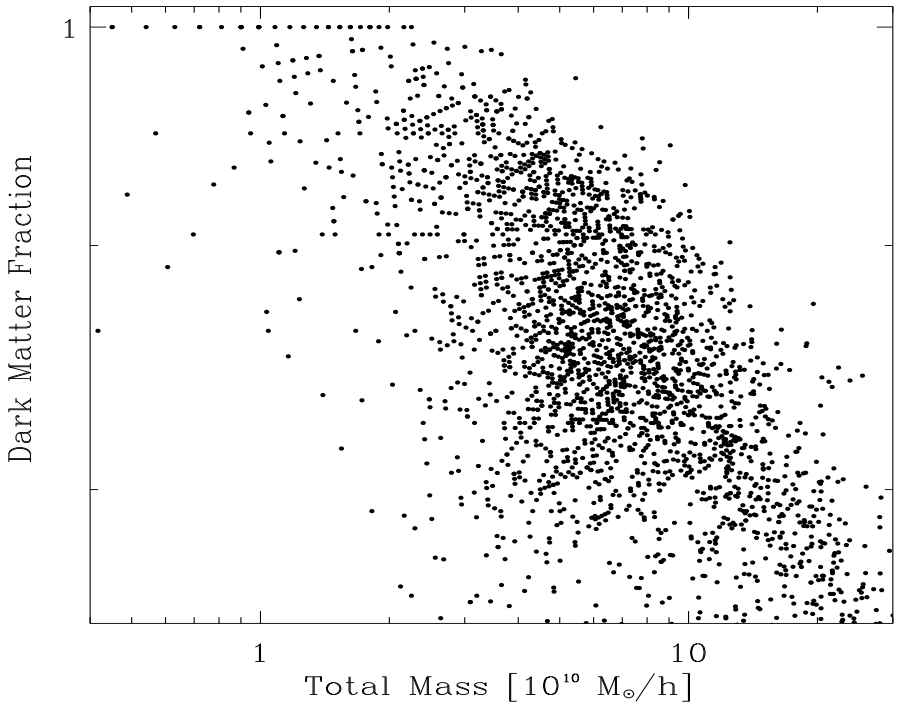

Figure 4.5: DM fraction versus total mass in the cluster of radius of 30 kpc and the minimum particle is 100

the stellar fraction is almost less than 30 percent. But when the total mass is increasing the stellar fraction is also increasing significantly. When the total mass is less than $5 \times 10^{10} M_0 h^{-1}$, the stellar fraction is decreasing, which is more dominated by DM halos. Still the concetration of stellar fraction is high in smaller mass cluster region as shown in Fig 4.9.

4. Gas fraction

   Gas fraction is determined by dividing the mass of gases in a cluster to the total mass. Its value is also less than 30 percent and has high concetration for smaller total mass of cluster, as shown in the Fig 4.10.

5. Baryon fraction

   Baryon mass is the sum of the mass of gas and star in a cluster. Inorder to determine baryon fraction, we divide the baryon mass to total mass in a given cluster. So the baryon fraction is less than 30 percent and the remaining will be as we expected DM and dark energy as shown in Fig 4.11.

6. Stars

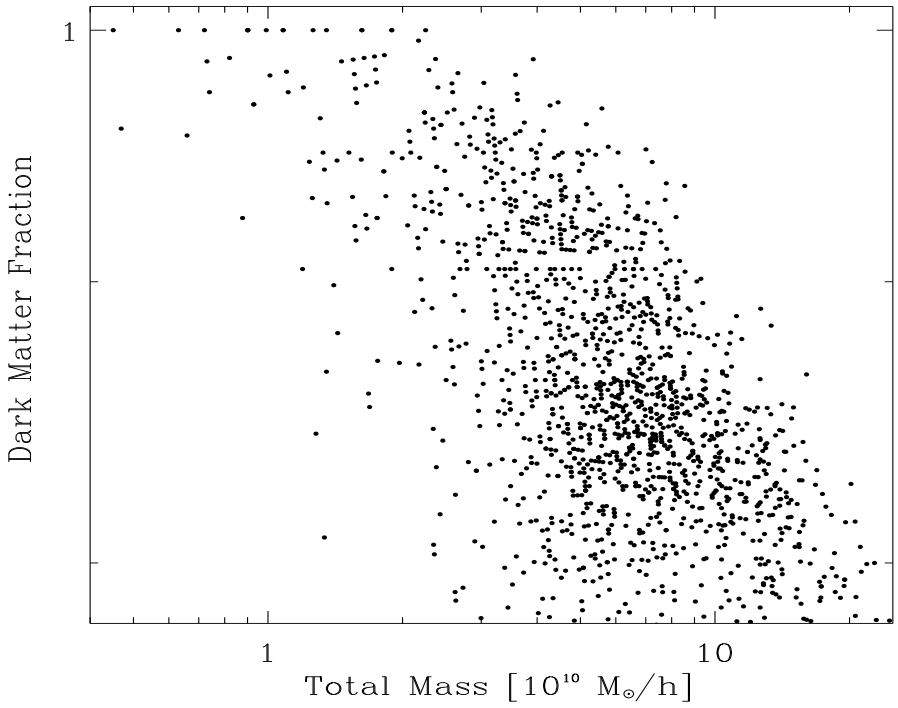

Figure 4.6: DM fraction for cluster 00281 with in the range of 30 kpc, the minimum number of particlicle is 100

In the ROCKSTAR halo finder we are searching the concentration and statistical distribution of stars by their mass, in which its number of particle is more than 100 and its radius from a given 3D coordinate center is 30 kpc. When we plotted a scatterd graph, using MareNostrum universe catalogue with ROCKSTAR sumilation code, we found that, its amount is linearly increasing with the mass of a cluster. But still the concetration of the halos are high in the lower total mass region of the cluster as shown in Fig 4.12.

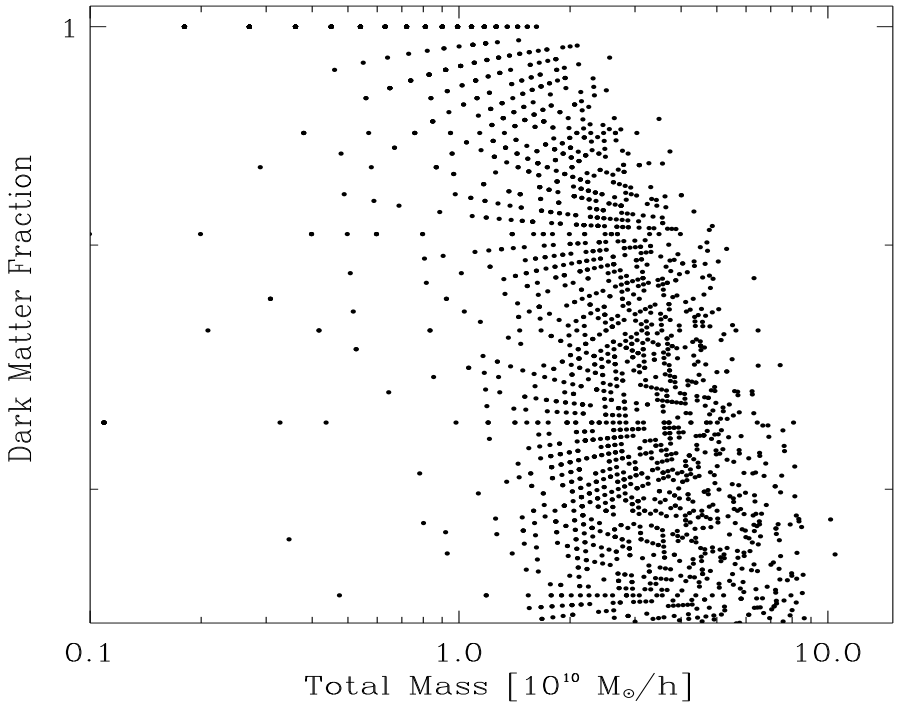

Figure 4.7: DM fraction for cluster number 00281 with in the radius 15 kpc and the minimum number of particle is 50

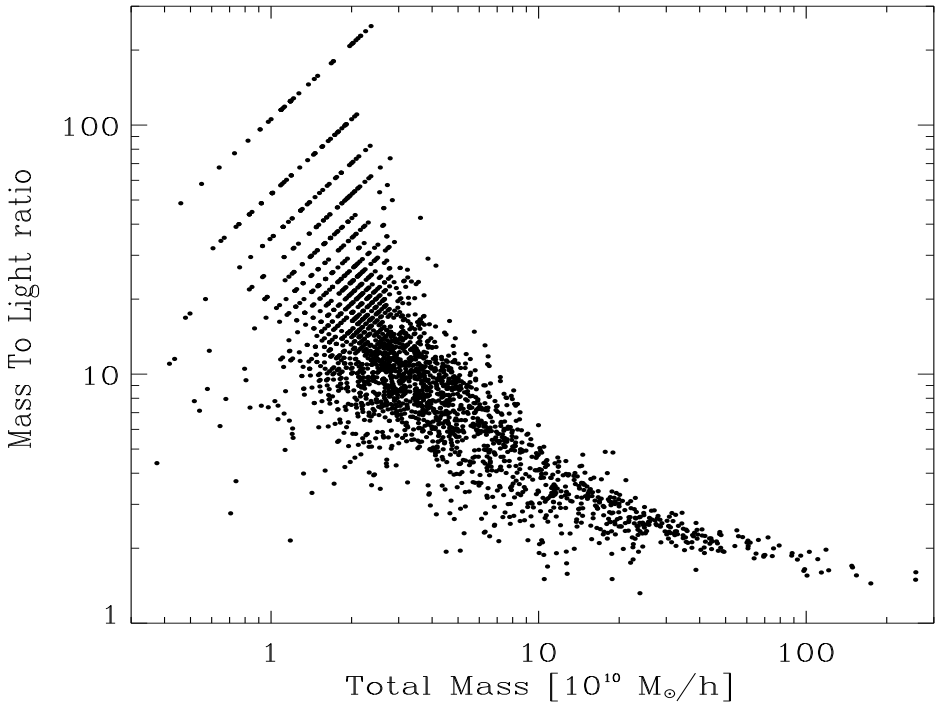

Figure 4.8: Mass to light ratio for cluster number 00281 with in the radius 15 kpc and the minimum number of particle is 50

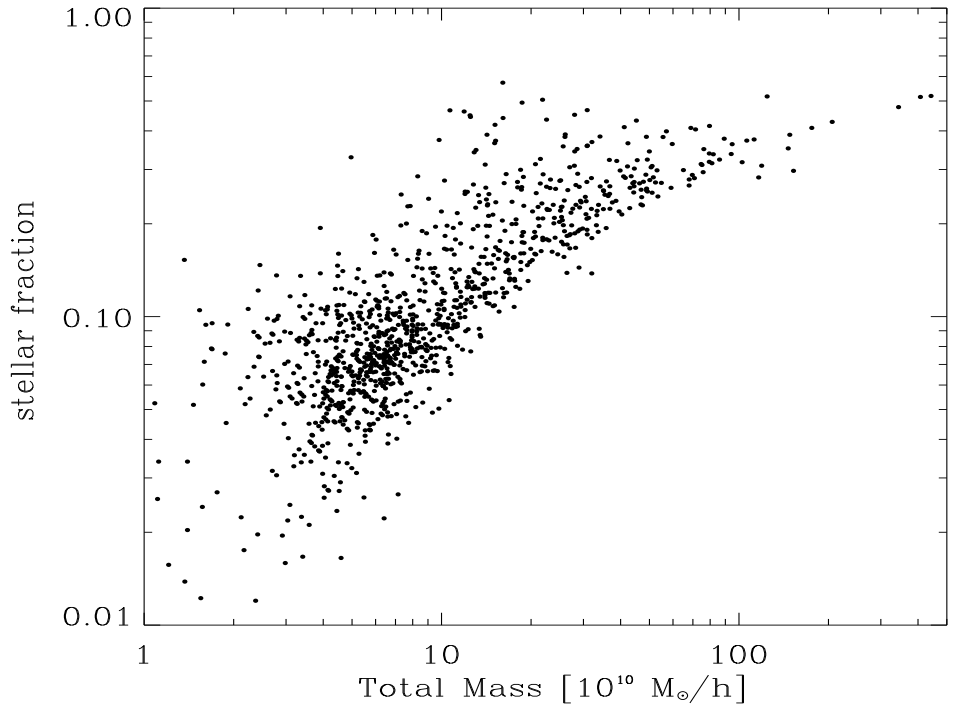

Figure 4.9: Stellar fraction versus total mass of the cluster with in 30 kpc

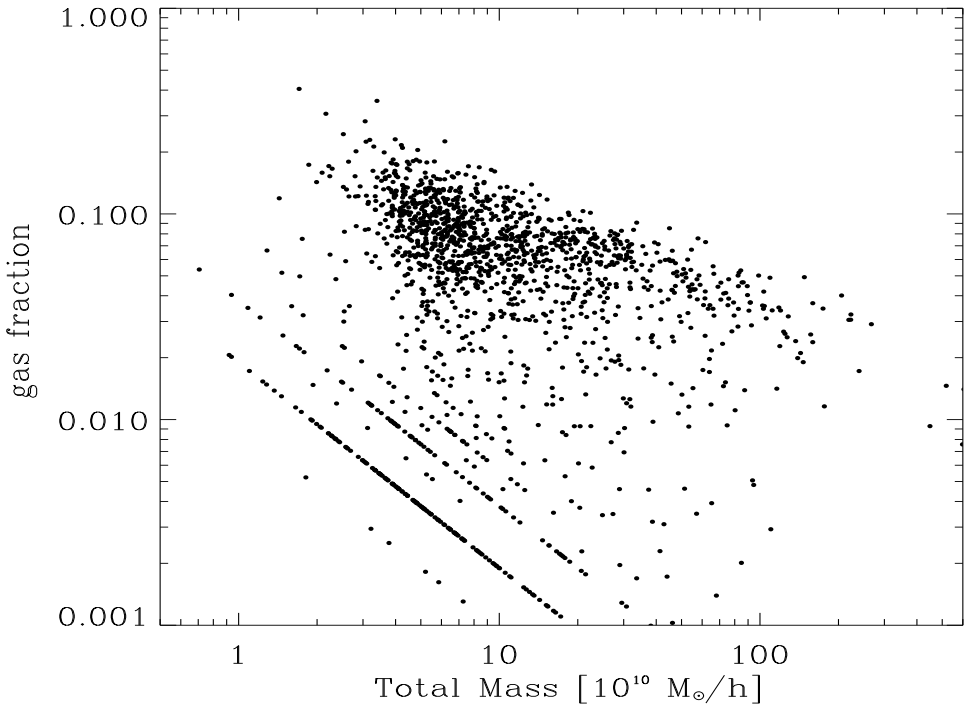

Figure 4.10: Gas fraction versus total mass for cluster 00142 with in 30 kpc

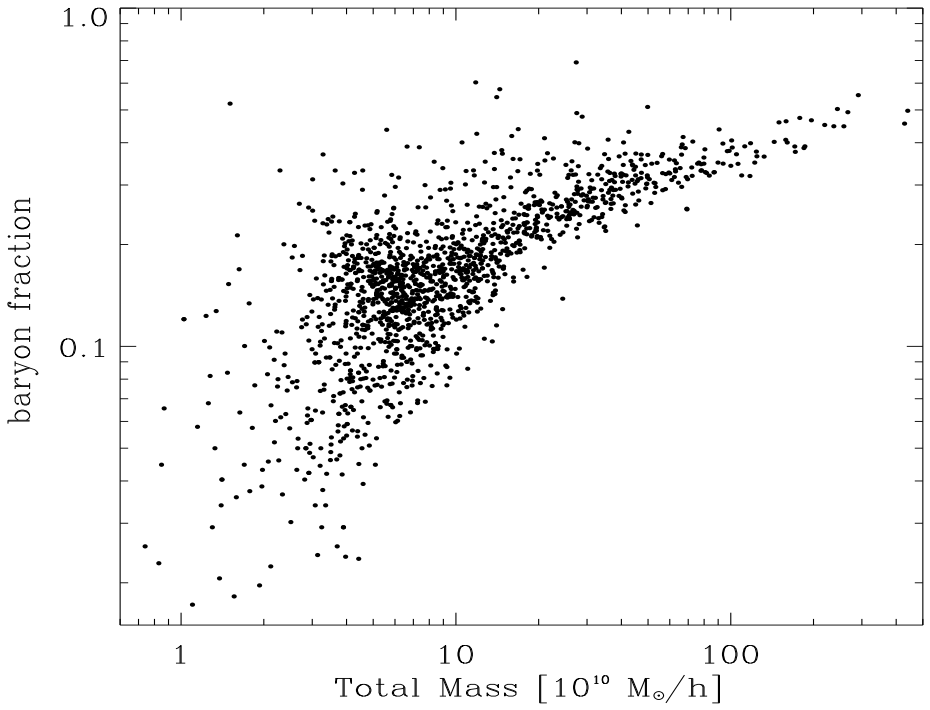

Figure 4.11: Baryon fraction versus total mass of the cluster with in 30 kpc

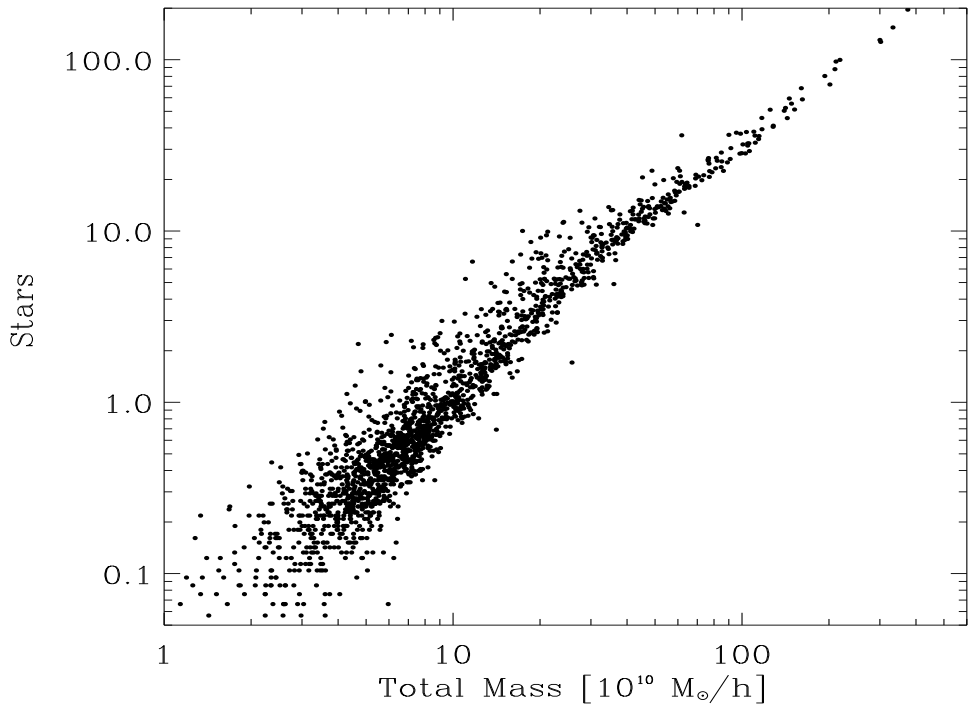

Figure 4.12: Stars versus total mass of cluster in 30 kpc radius and the minimum number of particle is hundred

CHAPTER 5
Conclusion

Galaxies are formed by the cooling and condensation of the baryonic gas trapped within the potential wells of virialized DM clumps (DM haloes). Galaxy cluster is one of the largest known gravitationally bound object in the universe, still there are huge super clusters in the universe. The galaxy clusters can be used as probes of structure and galaxy formation as they retain an imprint of how they were formed.

The masses of galaxies are found from the orbital motion of their stars. Stars in a more massive galaxy will orbit faster than those in a lower mass galaxy because the greater gravity force of the massive galaxy will cause larger velocity of its stars. As DM affects clusters, they are also valuable for measuring DM content in the universe. Structure formation theory suggests that DM is cold, i.e, moving non relativistically during structure formation. However, cold DM predicts many more DM satellites, or subhalos, around galaxies such as the Milky Way than observed.

DM and dark energy are the dominant part of our universe. There is strong evidence that more than 80% of all matter in the Universe is dark, it interacts very weakly with electromagnetic radiation and ordinary matter. The dominant component of this cosmological DM should be non-baryonic particles. Weakly interacting massive particles (WIMPs) χ arising in several extensions of the standard model of electro-weak interactions, are one of the leading candidates for DM. WIMPs are stable particles with masses roughly between $10GeV$ and a few TeV and interact with ordinary matter only weakly .

In this thesis, we focused on the statistical studies of DM dominated subhalo-s, with the help of ROCKSTAR simulation halo finder algorithm, we searched the content of subhalos which contain DM in the cluster. There are different halo finders such as Amiga halo finder (AHF) but my simulation is based on ROCKSTAR halo finder with its own linking length. Cosmological N-body simulations have been widely used to study the statistical distribution of halos and its subhalos, which have been used as an important tool for a better understanding of DM

content in the halos as well as subhalos and it also used to study the nonlinear structure formation of the universe.

Using marenostrum-multiDark simulation of galaxy Clusters, for 282 clusters in the ROCKSTAR simulation algorithm, there are 466621 halos, which contains more than 100 particles with a radius of $30kpc$. Each particle mass is assumed to be nearly equal to $10^7 M_0$. We also analyzed mass to light ratio, which helps to detrmine the DM content. Mass to light ratio is determind by dividing the total mass to the star mass. The number of subhalos whose mass to light ratio above one is around 132332, which means the concentration of DM in the given cluster is high. We also determine the mass to light ratio with respect to $\frac{r}{r_{200}}$. It is high with in the radius around $1 \times r_{200}$. So the DM content and its concetration is high around r_{200}, which satisfies its relic density.

In these simulation, we also depict the DM fraction, gas fraction, baryon fraction, and stellar fraction. When we Consider DM fraction, its distribution is high around $1\times10^{10}-10\times10^{10}M_0/h$. The Statistical distributon of DM sub haloes in these region is about 82%, so we conclude that the concetration of DM is high for the smaller mass of a cluster.

We also compare the DM fraction of the same cluster 00281, with differnt radius and number of particles. We take two cases, the first one is, 15 kpc radius and the minimum number of particle is 50. The second one is, 30 kpc radius and the minimum number of particle is 100. We justify that more subhalos are observed in 15 kpc than 30 kpc in the range of $1 \times 10^{10} - 10 \times 10^{10} M_0/h$ and its concetration is also high. Because the subhalo finder includes some outliers in the first case, which may not include in second case, so the probablity of finding subhalos in the first case is high.

When we consider gas fraction, baryon fraction and stellar fraction, their content in these simulation is less than 30%. So we justify that the DM content is dominant in these cluster, that is why the rotation curve of the cluster is affected by unknown matter, which we call it DM.

In super symmetric model extension of standard model, weakly interacting massive particles, the so called WIMPS are good candidates of DM. They can be present in the right amount to explain the unobserved matter density of the Universe. Neutralinos is the leading candidate for WIMP. It is stable and therefore may be left over after the Big Bang. They bound gravitationally with ordinary stars in the galactic halos, and in particular they are also present in our own galaxy, the

Milky Way. As a consequence there are a flux of these DM particles on the Earth. Axions, light gravitinos and sterile Nuetrinos are other candidates of DM. They have relic density in the universe, with thermal and non thermal production and their interaction with ordinary matter are also weak.

We also analyze the DM content using generalized Viral theorem in Brane $f(R)$ gravity, here we are trying to show that, the mass of DM is dominant in the universe. The viral mass is nearly equal to the total mass, which is the mass of DM.

In genral, the statistical distribution of DM is Gaussian distribution. It can be obtained by solving Poisson's equation.

Our future plan is to study the statistical distribution of DM in different criterion such as radius, number of particles and using different catalogue. Analayse the density field of the DM by means of a counts-in-cells method in a low-density cold DM (CDM) simulated universe and compare it using X ray emission data analysis of DM. Using Monte carlo simulation and gravitational lensing, we will try to determine the exact proportion of visible matter, DM and dark energy in the universe.

Bibliography

[1] Forero-Romero, Jaime E Gottlöber, and Stefan Yepes Gustavo. Bullet clusters in the marenostrum universe. *The Astrophysical Journal*, 725(1):598, 2010.

[2] Gondolo, Paolo and Edsjö, Joakim and Ullio, Piero and Bergström, Lars and Schelke, Mia and Baltz, Edward A. DarkSUSY: Computing supersymmetric dark matter properties numerically. *Journal of Cosmology and Astroparticle Physics*, 2004: 07, 008, 2004, IOP Publishing.

[3] Marchegiani, Paolo and Colafrancesco, Sergio. Is the radio emission in the Bullet cluster due to dark matter annihilation?. *Monthly Notices of the Royal Astronomical Society*, 452: 2, 1328–1340, 2015, The Royal Astronomical Society.

[4] Jonathan L Feng. Dark matter candidates from particle physics and methods of detection. *Annual Review of Astronomy and Astrophysics*, 48:495–545, 2010.

[5] Shin'ichiro Ando and Daisuke Nagai. Fermi-lat constraints on dark matter annihilation cross section from observations of the fornax cluster. *Journal of Cosmology and Astroparticle Physics*, 2012(07):017, 2012.

[6] Munoz, C. Dark matter detection in the light of recent experimental results 2004 Int. *J. Mod. Phys. A*, 19 : 3093, 2004.

[7] Chung Kao. Neutralino dark matter in supersymmetric models. National Central University, 2004.

[8] AS Sefiedgar, Z Haghani, and HR Sepangi. Brane-f (r) gravity and dark matter. *Physical Review D*, 85(6):064012, 2012.

[9] Michael Kuhlen, Mark Vogelsberger, and Raul Angulo. Numerical simulations of the dark universe: State of the art and the next decade. *Physics of the Dark Universe*, 1(1-2):50–93, 2012.

[10] Matthias Bartelmann and Peter Schneider. Weak gravitational lensing. *Physics Reports*, 340(4-5):291–472, 2001.

[11] Stuart Bowyer and Thomas W Berghöfer. Inverse compton scattering as the source of diffuse extreme-ultraviolet emission in the coma cluster of galaxies. *The Astrophysical Journal*, 506(2):502, 1998.

[12] Sergio Colafrancesco. Sz effect from dark matter annihilation. *Astronomy & Astrophysics*, 422(2):L23–L27, 2004.

[13] Yao-Yuan Mao. *Modeling the Distribution of Dark Matter and Its Connection to Galaxies*. PhD thesis, Stanford University, 2016.

[14] van den Bosch, Frank C, and Fangzhou Jiang. Statistics of dark matter substructure–ii. comparison of model with simulation results. *Monthly Notices of the Royal Astronomical Society*, 458(3):2870–2884, 2016.

[15] Dairbekov, Nurlan S and Sharafutdinov, Vladimir A. On conformal Killing symmetric tensor fields on Riemannian manifolds. *Siberian Advances in Mathematics*, 21: 1, 1–41, 2011, Springer.

[16] Klasen, Michael and Pohl, Martin and Sigl, Günter. Indirect and direct search for dark matter. *Progress in Particle and Nuclear Physics*, 85: 1–32, 2015, Elsevier.

[17] Ueda, Haruhiko and Yokoyama, Jun'ichi. Counts-in-cells analysis of the statistical distribution in an N-body simulated universe. *Monthly Notices of the Royal Astronomical Society*, 280: 3, 754–766, 1996, Blackwell Science Ltd Oxford, UK.

[18] Casas Miranda, Rigoberto Angel. Statistics of the Dark Matter Halo Distribution in Cosmic Density Fields *lmu*, 2002.

[19] Mannheim, Philip D. Alternatives to dark matter and dark energy. *Progress in Particle and Nuclear Physics*, 56: 2, 340–445, 2006, Elsevier.

[20] Yang, Lin. INVESTIGATIONS OF DARK MATTER USING COSMOLOGICAL SIMULATIONS. *Johns Hopkins University*, 2017.

[21] Kamionkowski, Marc. Dark matter and dark energy. *arXiv preprint arXiv:0706.2986*, 2007.

DECLARATION

ADDIS ABABA UNIVERSITY
COLLEGE OF NATURAL AND COMPUTATIONAL SCIENCES
DEPARTMENT OF PHYSICS

MSc Thesis

Statistical Studies of DM Dominated Subhalos

Name of Candidate:Kifelom Mehari

I the under signed declare that the thesis is my original work and no part of it can be claimed as an intellectual property of anybody else except me.

Signature: _____